Egyptian Journal of Aquatic Biology and Fisheries
Zoology Department, Faculty of Science,
Ain Shams University, Cairo, Egypt.
ISSN 1110 – 6131
Vol. 29(4): 3157 – 3190 (2025)
www.ejabf.journals.ekb.eg

Biometric Relationships of the Bivalve *Mactra stultorum* and Bioactivities of Its Chitosan-Based Nanoparticles

Somaia M. Zakzok[1], Hala E. Abd-Alaty[1], Nasser M. Hosny[2], Mohamed M. Tawfik[1*]

[1]Zoology Departement, Faculty of Science, Port Said University, Egypt
[2]Chemistry Departement, Faculty of Science, Port Said University, Egypt

[*]**Corresponding Author: tawfik@sci.psu.edu.eg**

ARTICLE INFO

Article History:
Received: June 30, 2025
Accepted: Aug. 18, 2025
Online: Aug. 27, 2025

Keywords:
Mactra stultorum,
Chitosan,
Biometric,
Anticancer,
Antioxidants,
Anti-inflammatory

ABSTRACT

Marine bivalve molluscs represent a key functional group in marine ecosystems. In the present study, the shell morphology of *Mactra stultorum* (length, width, and height) was examined alongside the synthesis, characterization, and biological evaluation of its chitosan (CS) and CS–CuO nanocomposite. Both chitosan and CuO nanoparticles are known for their diverse biological effects. The CS–CuO nanocomposite was synthesized using a co-precipitation method and was characterized by infrared spectroscopy (IR), X-ray powder diffraction (XRD), and transmission electron microscopy (TEM). IR spectra confirmed the loading of CS onto CuO, XRD analysis demonstrated the formation of monoclinic CuO nanoparticles, and TEM images revealed CuO quantum dots with an average size of ~5 nm. Biological assays showed that CS, CuO, and CS–CuO nanoparticles exhibited strong antiproliferative activities against several cancer cell lines. CS–CuO displayed the highest activity against HepG2 cells (IC_{50} = 19.81 µg/mL), while CS showed superior activity against HCT-116 and MCF-7 cells (IC_{50} = 14.71 and 21.27 µg/mL, respectively), as determined by MTT assay. Both CS and CS–CuO nanoparticles demonstrated marked antimicrobial activity (24–77%) against six different microorganisms. In addition, all tested compounds exhibited potent antioxidant effects in a dose-dependent manner, effectively scavenging DPPH and nitric oxide radicals and reducing ferric ions. Furthermore, CS and CS–CuO nanoparticles inhibited cyclooxygenase-2 (COX-2) activity, with inhibition rates of 61.27% and 52.31%, respectively, at 1.0mg/ mL. Overall, the findings highlight the potential bioactivity of chitosan and its nanocomposites derived from *Mactra stultorum*, suggesting promising applications in pharmaceutical and biomedical fields, while also reflecting potential non-ideal environmental conditions for this edible bivalve.

INTRODUCTION

Bivalves are filter feeders that are widely distributed worldwide in different aquatic ecosystems with about 15,000 species **(Mesquita *et al.*, 2023)**. Their high filtration ability gives a key ecological role in light penetration, water quality improvement, bioremediation processes as well as nutrient and carbon cycles **(Ferreira**

***et al*., 2014; Mesquita *et al*., 2023)**. In addition to their significant ecological benefits, marine bivalves are considered as a healthy food since they are enriched with omega-3 fatty acids, minerals, proteins as well as essential vitamins that significantly impact human well-being **(Wijsman *et al*., 2019)**. Moreover, these edible organisms are valuable sources of potent bioactive molecules that possess anticancer, antioxidant in addition to antibacterial activity **(Hasan *et al*., 2016; Odeleye *et al*., 2016; Chai *et al*., 2017; Chernikov *et al*., 2017)**. *Mactra stultorum* (Linnaeus 1758) is an abundant benthic bivalve species that is related to family Mactridae **(Derbali *et al*., 2021)**. This edible clam is one of the most commercial species along the Mediterranean coast in Port Said, Egypt.

Chitin is the most abundant aminopolysaccharide polymer in nature and serves as a major structural component of the exoskeletons of many invertebrates, particularly the shells of bivalves **(Elieh-Ali-Komi & Hamblin, 2016)**. It provides support and strength to withstand the harsh conditions in their environment in addition to its immune responses against different types of pathogens and microbes **(Lee *et al*., 2011; Hahn *et al*., 2020)**. Chitosan is a naturally occurring biopolymer obtained through the deacetylation of chitin, comprising repeating units of glucosamine and N-acetylglucosamine **(Perelshtein *et al*., 2013; Souza *et al*., 2020)**. Chitosan has gained considerable interest in the biomedical and pharmaceutical sectors because of its wide availability, low production cost, non-toxic nature, biodegradability, and high biocompatibility **(Barreto *et al*., 2017; Adhikari & Yadav, 2018)**. Moreover, chitosan exhibits powerful antimicrobial activities that can suppress the growth of a panel of bacteria by the electrostatic interaction between its positively charged moieties and the negatively charged groups present on the surface of on microbial membranes **(Adhikari & Yadav, 2018; Ahmed *et al*., 2021)**.

Nanotechnology is a rapidly developing area of scientific research concerned with the synthesis and development of small particles called nanoparticles that possess significantly unique chemical, physical and biological properties because of their small size (10- 100nm) **(Gouda & Hebeish, 2010; Syame *et al*., 2017)**. Recently, using of nanotechnology and polymers together has gained a great attention in different fields especially therapeutic innovation and pharmaceutical industry **(Agarwal *et al*., 2018)**. Over recent years, metal oxide nanoparticles are considered as an interesting solution to enhance the biological activities of the biopolymers due to their unique nanoscale surface properties, excellent synergistic effects and potential applied aspects **(AbdElhady, 2012; Covarrubias *et al*., 2018)**. Copper oxide is among the most metal oxide nanoparticles with specific chemical and physical properties that have attracted much attention to be used in water treatment and food packages since they are effective antibacterial agents **(Lastovina *et al*., 2016; Syame *et al*., 2017; Covarrubias *et al*., 2018)**.

Currently, chitosan nanoparticles are extensively utilized in various biomedical fields, including drug delivery, wound healing, tissue engineering, and stem cell

technology, owing to their antimicrobial, anticancer, anti-inflammatory, and anti-obesity properties **(Azuma *et al*., 2014; Adhikari & Yadav, 2018; Ahmed *et al*., 2021)**.

The aim of this work was to invesigate some biological information of the edible clam *M*. *stultorum* collected from Port Said, as well as synthesizing and characterizing chitosan-copper oxide nanoparticles. The present study was also conducted to evaluate and compare the biological activities (anticancer, antimicrobial, antioxidant, and anti-inflammatory) of chitosan (CS), copper oxide (CuO), and chitosan-copper oxide nanoparticles (CS-CuO NPs).

MATERIALS AND METHODS

Samples collection and measurements

A total of 250 *Mactra stultorum* individuals were sampled from the Mediterranean coast in Port Said, Egypt. Measurements of shell length (SL), width (SWi), and height (SH) were taken with a Vernier caliper to an accuracy of 0.01mm. Shell weight (SWt) and total body weight (TWt) were determined using a digital balance.

Biometric relationships

The biometric relationships were performed according to **Teissier (1948)** as the following:

1. **Shell length-shell height/width relationship**

The biometric relationships between SL and either of SH and SWi were calculated separately by testing each pair of variables using the following equations:

$$SH = a + b\ SL$$

$$SWi = a + b\ SL$$

Where, SH is shell height in mm, SL is shell length in mm, SWi is shell width in mm, “a” is a constant (the intercept of the regression line) and “b” is the regression coefficient (slope).

2. **Shell length-shell weight relationship**

The following equation was used to calculate this relationship:

$$SWt = a\ SL^{b}$$

Where, SWt is shell weight in grams, SL is shell length in mm, “a” is a constant or intercept and “b” is the slope.

3. **Shell length-total body weight relationship**

This relationship was estimated by the following equation:

$$TWt = a\ SL^{b}$$

Where, TWt is total body weight in grams, SL is shell length in mm, “a” is a constant or intercept and “b” is the slope.

Chitosan extraction

The extraction of chitosan from *M. stultorum* shells involved three main processes: demineralization, deproteination and deacetylation **(Thomas *et al.*, 2015)**. Briefly, the shells were incubated in 2M hydrochloric acid at the ratio of 10:1 (weight/volume "w/v") at room temperature for 24h in order to be demineralized. After that, shells were thoroughly washed and were then treated with a 2% NaOH solution until a neutral pH was attained. Deproteination process was carried out by the immersion of the demineralized shells in 10% NaOH solution with solvent to solid ratio of 1:15 (w/v) at 70°C for 2h. After cooling at room temperature, the deproteinized product was deacetylized with 50% NaOH solution with 10:1 ratio (w/v) in a water bath shaker, then filtered and washed using distilled water until pH 7. The solid matter (chitosan) was finally dried at 80°C in an electric oven for 3h, and then crushed by using a blender to obtain chitosan powder.

Synthesis of chitosan-copper oxide nanoparticles (CS-CuO NPs)

NaOH (3.2g) was added to copper acetate (7.9 g) dissolved in 100mL distilled water, followed by stirring the mixture for 12h at room temperature, before adding chitosan (2g dissolved in acetic acid). The previous mixture was subjected to further stirring for another 24h. The resulting precipitate was filtered off and dried at 60°C.

Characterization of chitosan-copper oxide nanoparticles

1. **Fourier transform infrared (FTIR) spectroscopy**

Both chitosan (CS) and chitosan loaded onto CuO nanoparticles (CS-CuO NPs) were analyzed using FTIR spectroscopy in order to investigate the formation of nanoparticles. In addition, this analysis was performed mainly to identify the specific biomolecules responsible for stabilizing and capping CuONPs. This test depends mainly on KBr pellet technique that includes mixing KBr salt with samples and then followed by the analysis using Perkin Elmer Spectrum BX FT-IR system in the range of 400–4000 cm^{-1} **(Lingaraju *et al.*, 2019)**.

2. **X-ray diffraction (XRD)**

The XRD analysis was performed to ensure the presence of copper atoms in the formed nanoparticles. This experiment was performed using monochromatized CuKα radiation (1.541 Aº) by X-ray diffractometer system (XPERT-PRO) operating at 40 kV and 40 mA. The scanning was continuous and time per step was 0.6 S.

3. **Transmission electron microscopy (TEM)**

The morphological properties of nanoparticles such as surface texture, size, dispersed state as well as shape were evaluated using high-resolution transmission electron microscopy (HRTEM, Philips CM-20) operating at 200 kV with magnification power of 469.13 KX at scales of 10 and 100 nm.

Anticancer activities

MTT (3-[4,5-dimethylthiazol-2-yl]-2,5-diphenyltetrazolium bromide) was used to evaluate the *in vitro* anticancer activities of CS, CuO, and CS-CuO nanoparticles, as

described by **Mosmann (1983)**. Three human cancer cell lines— liver (HepG2), colon (HCT-116) and breast (MCF-7)—along with normal human lung fibroblasts (WI-38), were obtained from the Holding Company for Biological Products and Vaccines (VACSERA), Cairo, Egypt. Cells were maintained in RPMI-1640 culture medium enriched with 10% heat-inactivated fetal bovine serum (FBS) and 1% penicillin. Cultures were incubated at 37°C under a humidified environment with 5% CO_2 to support optimal growth conditions After that, cells were seeded on 96 plates (1×10^4 cells/well) for 25h, and then each compound was added to the cells with serial concentrations (1.56-100µg/ mL). After 48h of treatment, MTT dye dissolved in a fresh medium (10 µL/well) was added to cells and was incubated at 37°C for 4h to permit the formation of formazan crystals in viable cells only. The dissolution of these crystals was achieved by dimethyl sulfoxide (DMSO, 100µL/ well). Finally, the absorbance was measured at a wavelength of 570nm using a Bio-Tek microplate reader (EXL 800, USA). Doxorubicin was employed as the positive control, while untreated cells served as the negative control. The percentage of cell viability was determined using the following equation:

$$\text{Cell viability (\%)} = 100 \times (A_{570} \text{ of treated cells} / A_{570} \text{ of untreated cells}).$$

The half-maximal inhibitory concentration (IC_{50}) for each treatment was determined by analyzing dose–response curves, plotting dose concentration on the X-axis against the percentage of cell inhibition on the Y-axis, using GraphPad Prism version 8.0.1 (244).

Antimicrobial activities

The *in vitro* antimicrobial activity of the tested compounds was assessed against two Gram-negative bacteria (*Escherichia coli* and *Pseudomonas aeuroginosa*), two Gram-positive (*Staphylococcus aureus* and *Bacillus subtilis*) in addition to two fungal species (*Candida albicans* and *Aspergillus flavus*) using disc diffusion method **(Bauer *et al*., 1966; Mercan *et al*., 2006)**. Briefly, sterilized paper discs with standard size (5cm) were soaked in 1.0mg/ mL of each treatment and were seeded aseptically in sterilized petri dishes that contain nutrient agar media (20g agar, 3g beef extract as well as 5g peptone) with each microbe species. Then, the plates were incubated under favorable conditions of each tested microorganisms. Ampicillin was used as a standard antibiotic and Colitrimazole was considered as a standard antifungal agent. While, DMSO represents a negative control. Following incubation, the diameter of each inhibition zone (in millimeters) was measured to represent the antimicrobial efficacy and the activity index (%) for each compound was estimated using the following formula:

Activity index (%) = (Inhibition zone's diameter of each tested compound / inhibition zone's diameter of positive control) ×100.

Antioxidant activities

1. **DPPH radical scavenging assay**

The *in vitro* antioxidant activity of each compound was evaluated using the 1,1-diphenyl-2-picrylhydrazyl (DPPH) radical scavenging assay, following the protocol

described by **Brand-Williams *et al.* (1995)** with slight modifications. In summary, a 0.1 mM DPPH solution prepared in 95% methanol was mixed with several concentrations (0.01– 0.1mg/ mL) of each tested compound and incubated at room temperature for 30 minutes. Ascorbic acid (vitamin C) was used as the positive control. Absorbance was measured at 517nm using a UV-VIS spectrophotometer (Milton Roy), and the percentage of scavenging activity was estimated using the following formula:

DPPH radical scavenging activity (%) = [(blank absorbance – samples or standard absorbance) / blank absorbance] × 100.

The IC_{50} values (the concentration of each treatment inhibits 50% of DPPH free radicals) were calculated using the log dose inhibition curve using GraphPad Prism 8.0.1 (244).

2. Ferric reducing antioxidant power (FRAP)

The potential antioxidant capacity of the tested samples was evaluated using the FRAP assay, as described by **Oyaizu (1986)**. This method is based on the ability of each sample to reduce ferric ions (Fe^{3+}) to ferrous ions (Fe^{2+}). Briefly, 1.0mL of methanolic solution containing varying concentrations of the samples (0.016 to 1mg/ mL) was mixed with 2.5mL of sodium phosphate buffer (0.2M, pH 6.6) and 2.5mL of potassium ferricyanide [$K_3Fe(CN)_6$]. The mixture was incubated for 20 minutes at 50°C, after that the pH was reduced to 3.6 by adding 2.5mL of trichloroacetic acid. The resulting solution was centrifuged at 1000 ×*g* for 10 minutes. Subsequently, equal volumes (2.5mL) of the supernatant and deionized water were combined with 0.5mL of freshly prepared ferric chloride. Vitamin C (Ascorbic acid) was utilized as the reference standard. Absorbance was measured at 593nm using a UV-VIS spectrophotometer (Milton Roy). The ferric reducing capacity (%) was calculated using the formula:

Ferric reducing capacity (%) = [(Absorbance of control - Absorbance of samples or standard) / Absorbance of control] × 100.

The IC_{50} values were determined from the dose response curve using GraphPad Prism 8.0.1 (244).

3. Nitric oxide (NO) radical scavenging assay

Scavenging activities of CS, CuO and CS-CuO NPs for NO radicals were evaluated using sodium nitroprusside (SNP) as described by **Marcocci *et al.* (1994)**. The reaction mixture (3 mL) containing 10 mM SNP, serial concentrations of all tested samples or standard and Phosphate-buffered saline (PBS, pH 7.4) was incubated for 150 minutes at 25 °C. Following incubation, 1.0 mL of Griess reagent—comprising 1% (w/v) sulphanilamide dissolved in 5% (v/v) phosphoric acid and 0.1% naphthyl ethylenediamine dihydrochloride—was added to 0.5mL of the reaction mixture and further incubated for 30 minutes at 25°C. Nitrite levels were quantified by measuring absorbance at 546nm against an appropriate blank (excluding sodium nitroprusside, SNP) and a reference standard (vitamin C). All experiments were carried out in triplicate for

each tested sample. The inhibition percentage was determined using the following equation:

Inhibition (%) = [(Absorbance of blank – Absorbance of samples or standard) / Absorbance of blank] × 100.

The IC_{50} values of all tested samples were calculated from the concentration inhibition response curve using GraphPad Prism 8.0.1 (244).

4. Anti-inflammatory activities (cyclooxygenase "COX"-2 inhibition assay)

The ability of CS, CuO, and CS-CuO NPs to inhibit COX-2 activity is used as an indication of their potential anti-inflammatory effect **(Larsen *et al.*, 1996)**. In the presence of hematin, different concentrations of each tested sample or standard (0.016-1 mg/mL) were pre-incubated with COX-2 enzyme for 5 minutes at room temperature. The enzyme mixture was then mixed with 50μM arachidonic acid, 500 μM Phenol, 20 μM 1-leuco-dichlorofluorescein, and 1.0 mL Tris-buffer (0.1 M, pH 8). Nordihydroguairetic acid (NDGA) was considered as a standard and the reaction mixture without enzyme represented the blank. The absorbance was measured using a Milton Roy spectrophotometer within 15 seconds at 502nm. The IC_{50} value (mg/mL), which is the concentration of each tested sample or standard that inhibited 50% of cyclooxygenase, was estimated from the concentration inhibition curve.

Statistical analysis

All experiments were designed in triplicates (n = 3). The data were represented as mean ± standard deviation (SD). Statistical analysis was carried out using One-way ANOVA followed by the Tukey's test (SPSS version 22). When the *P*-value was less than 0.05, a statistically significant difference was reported.

RESULTS

Biometric relationships

The biometric relationship between shell lengths with width, height and both shell and total weights of *Mactra stultorum* are shown in Table (1). The relationships between SL and either of SH and SWi showed negative allometric growth patterns, where b values were less than 1 (0.6758 and 0.361, respectively). Similarly, a negative allometric growth was observed between SL and SWt as b value was less than 3 (2.6967). However, the relationship between SL and TWt showed a positive allometry growth, as b value was larger than 3 (3.0112). Regression equations and correlation coefficients of *Mactra stultorum* are shown in Table (1).

Table 1. Regression equations, correlation coefficient (R^2), b value and mode of growth of *Mactra stultorum.* SL: shell length, SH: shell height, SWi: shell width, SWt: shell weight and TWt: total weight

Relationship	Regression equation	R^2	b values	Growth patterns
SL-SH	SH= 0.6758 SL + 1.4323	0.8016	0.6758	–ve
SL-SWi	SWi = 0.361 SL + 2.4506	0.2683	0.361	–ve
SL-SWt	$SWt= 0.0002\ SL^{2.6967}$	0.7916	2.6967	–ve
SL-TWt	$TWt= 0.0001\ SL^{3.0112}$	0.8098	3.0112	+ve

Characterization of chitosan-copper oxide nanoparticles

1. **Fourier transform infrared (FTIR) spectroscopy**

Infrared spectra of both free chitosan (CS) and the chitosan loaded onto CuO (CS-CuO) nanoparticles (Fig. 1) were carried out to support the loading of CS on the surface of the nanoparticles through comparing the characteristic groups of chitosan in the two samples.

The spectrum of the free chitosan in KBr disc shows a broad band centered at 3450 cm^{-1} due to the stretching vibrations of the hydroxyl groups' ν (OH). It also exhibits broad bands with shoulders in the region 3300- 3222cm^{-1}. The spectrum of CS-CuO (Fig. 1) exhibits the stretching vibrations bands of the hydroxyl and amino groups in their positions as the free (CS) with slight shifts. This band was shifted to 1576 cm^{-1} and became much sharper in the spectrum of CS-CuO composite as it may be coordinated the metal oxide nanoparticles. Bands were shifted to 1185 and 1017cm^{-1}, respectively, in the spectrum of (CS-CuO) suggesting the binding of (CS) to (CuO).

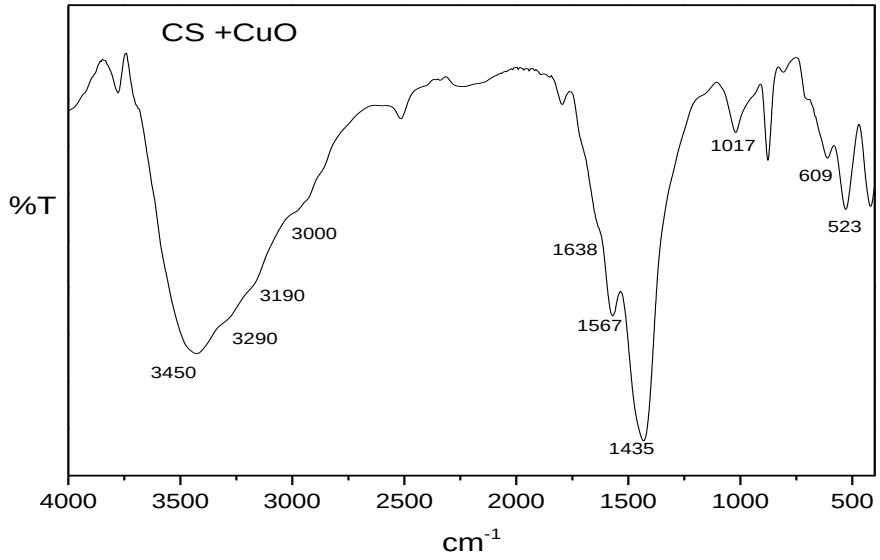

Fig. 1. IR spectrum of CS-CuO nanoparticles

2. X-ray diffraction (XRD)

To confirm the formation of CuO nanoparticles and their incorporation with chitosan, the XRD pattern of the CS–CuO nanocomposite was recorded (Fig. 2). The diffraction pattern exhibited characteristic peaks of CuO at 2θ values of 29.2°, 32.4°, 35.4°, 38.3°, 46.8°, 48.4°, and 52.7°, corresponding to the (110), (11), (002), (111), (102), (112), and (202) planes, respectively. These peaks are consistent with the standard diffraction data for monoclinic CuO crystals (JCPDS card no. 45–0937), confirming the crystalline phase. The lattice parameters of the monoclinic CuO crystal were calculated as a = 4.685 Å, b = 3.425 Å, and c = 5.130 Å.

The average crystallite size was estimated using the Scherrer equation **(Klug & Alexander, 1974)**, based on the diffraction peak at 2θ = 38.3°, and was found to be approximately 12nm.

.

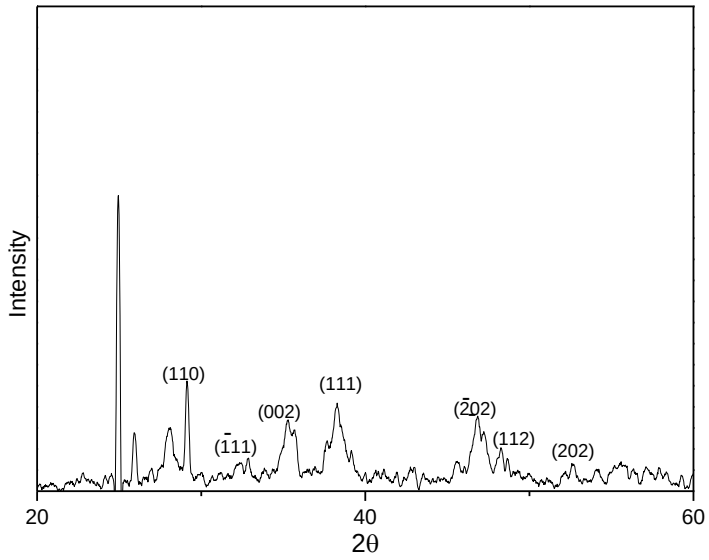

Fig. 2. XRD of CS-CuO nanoparticles

3. Transmission electron microscopy (TEM)

TEM image (Fig. 3) indicates that, chitosan aided the formation of quantum dots with sizes in the range 4- 10nm by coating and stabilizing the formed nanoparticles. It is clear that, the quantum dotes are collected in colonies with irregular spherical shapes. It is clear also, that the distribution of chitosan onto CuO is not homogenous and it forms sticks shapes like.

Anticancer activities

After treatment of the three human cancer cell lines (HCT-116, HepG2 and MCF-7) with CS, CuO and CS-CuO NPs for 48h, the growth inhibition of the cells was resulted in a dose-dependent pattern (Fig. 4). Overall, CS possessed significant higher cytotoxicity effect than other two compounds against HCT-116 and MCF-7 cells (P<0.001) with IC_{50} values are14.71±1.2 and 21.27±2.42 µg/mL, respectively, compared to these of CuO (75.33±1.84 and 87.4±2.11 µg/mL) and CS-CuO NPs (43.61±2.15 and 34.25±1.46 µg/mL) (Table 2). While, CS-CuO NPs exhibited significant higher anticancer activity against HepG2 cells (IC_{50}: 19.81±2.15 µg/mL) than that of CS and CuO (IC_{50}: 39.27±2.58 and 66.57±2.11 µg/mL, respectively) (P<0.001). However, less cytotoxic effects against normal lung cells (WI-38) were detected following the treatments with either tested compounds with IC_{50} values of 97.76±2.14, 95.72±1.01 and 87.44±2.14 µg/mL for CS, CuO and CS-CuO NPs, respectively. The assessment of the Selectivity Index (SI) value displays that CS was the most selective compound toward the cancer cells with a SI range 2.48-6.62, compared to the normal WI-38 cells. While, CuO and CS-CuO NPs have less SI ranges between 1.09-1.26 and 2-4.41, respectively (Table 2).

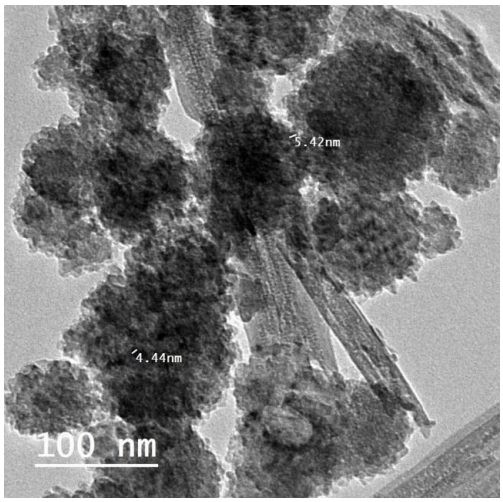

Fig. 3. TEM image of CS-CuO nanoparticles

Table 2. IC_{50} values and selectivity index (SI) of CS, CuO and CS-CuO NPs against HCT-116, HepG2, MCF-7 and WI-38 cells

	IC_{50} µg/mL				**Corresponding SI**		
	HCT-116	**HepG2**	**MCF-7**	**WI-38**	**WI-38 / HCT-116**	**WI-38 / MCF-7**	**WI-38 / MCF-7**
CS	14.71±1.2	39.27±2.58	21.27±2.42	97.76±2.14	6.62	2.48	4.59
CuO	75.33±1.84	66.57±2.11	87.4±2.11	95.72±1.01	1.27	1.43	1.09
CS-CuO NPs	43.61±2.15	19.81±2.15	34.25±1.46	87.44±2.14	2	4.41	2.55

IC_{50} data of CS, CuO and CS-CuO NPs are represented as means ± SD.

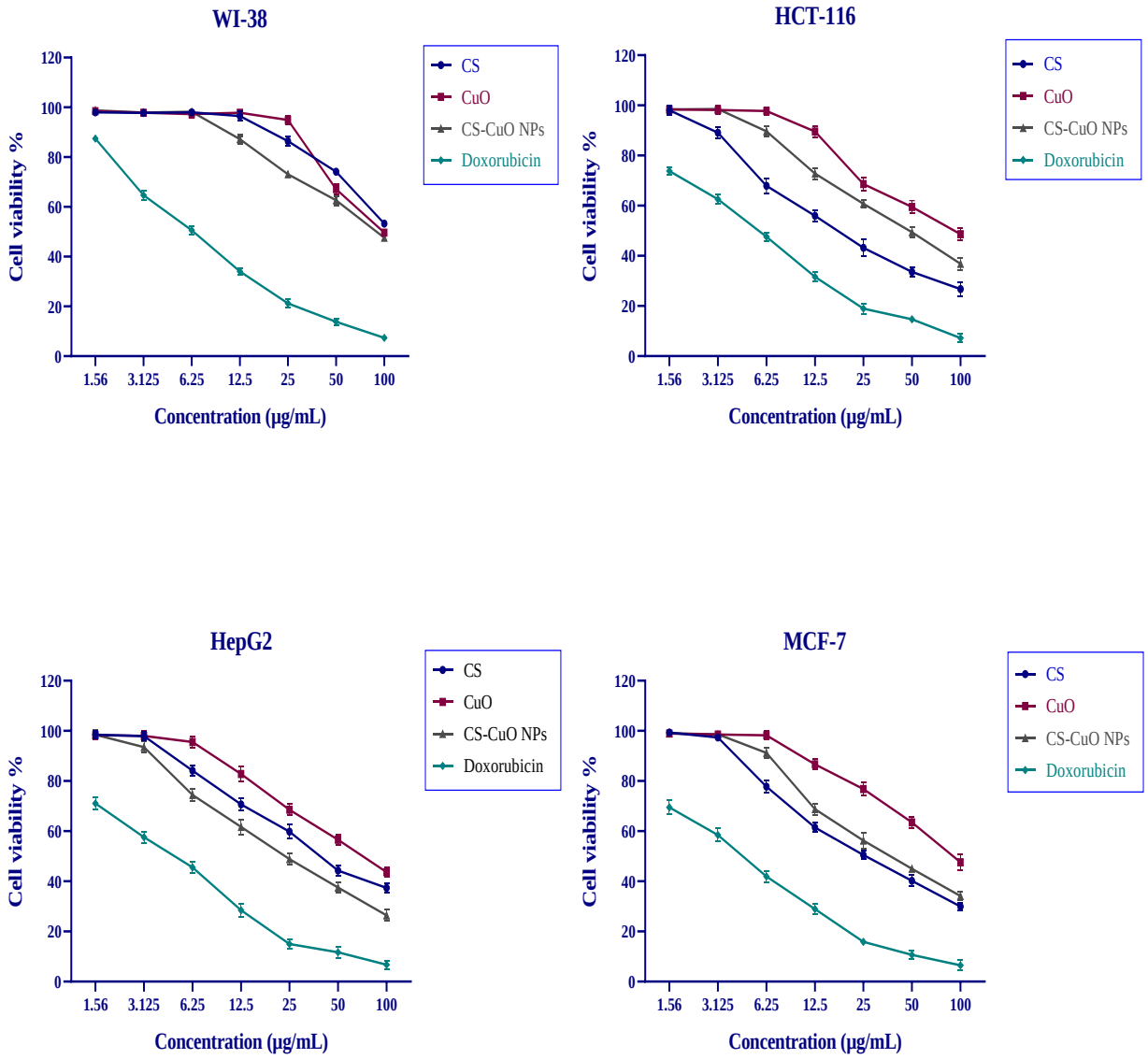

Fig. 4. The cytotoxicity of chitosan (CS), copper oxide (CuO), and chitosan–copper oxide nanoparticles (CS-CuO NPs), evaluated against various human cell lines, including normal lung fibroblasts (WI-38) and cancer cell lines (HCT-116, HepG2, and MCF-7). Cells were exposed to serial concentrations (1.56–100 µg/mL) of each compound for 48 hours. Doxorubicin was used as a positive control. Data are represented as the mean ± standard deviation (SD)

Antimicrobial activities

Both CS and CS-CuO NPs exhibited remarkable antimicrobial effects against six different microorganisms (two Gram-negative and two Gram-positive bacteria in addition to two fungal species). Regarding the antibacterial activity, CS showed a significantly

higher activity than that of CuO and CS-CuO NPs (P<0.05) (Fig. 5). CS inhibited more than 60% and 69% of the bacterial growth of *P. aeuroginosa* and *B. subtilis*, respectively (Table 3). The highest antibacterial activity of CS and CS-CuO NPs was observed against *B. subtilis* with inhibition zones of 16 and 12mm, respectively, while the minimum activity was recorded against *E. coli* with 10 and 6mm inhibition zones, respectively. Additionally, CS exhibited antibacterial effect as twice as CS-CuO NPs against *S. aureus*. On the other hand, CS-CuO NPs possessed the highest antifungal activity than other tested compounds (P<0.05) with significant largest inhibition zones (21 and 17mm) against *C. albicans* and *A. flavus*, respectively (Fig. 6). The growth of more than 68% of these fungal species was inhibited by using CS-CuO NPs (Table 3). Moreover, CS-CuO NPs showed relatively similar antifungal effect against *C. albicans* as that of Colitrimazole with 21 and 27mm inhibition zones in turn. However, CS exhibited moderate antifungal properties with same inhibition zone (13mm) against both tested fungi. Overall, CuO possessed the least antibacterial and antifungal activities among the tested compounds with no effect on *E. coli* (Table 3).

Table 3. Antimicrobial activity index percentage of CS, CuO, and CS-CuO NPs against four bacterial and two fungal species

	Antibacterial activity index (%)				**Antibacterial activity index (%)**	
	S. aureus	***B. subtilis***	***E. coli***	***P. aeuroginosa***	***C. albicans***	***A. flavus***
CS	50%	69.6%	40%	60.9%	48.1%	52%
CuO	8.3%	21.7%	NA	13%	22.2%	12%
CS-CuO NPs	29.2%	52.2%	24%	43.5%	77.8%	68%
Ampicillin	100%	100%	100%	100%	NA	NA
Colitrimazole	NA	NA	NA	NA	100%	100%

NA: not applicable

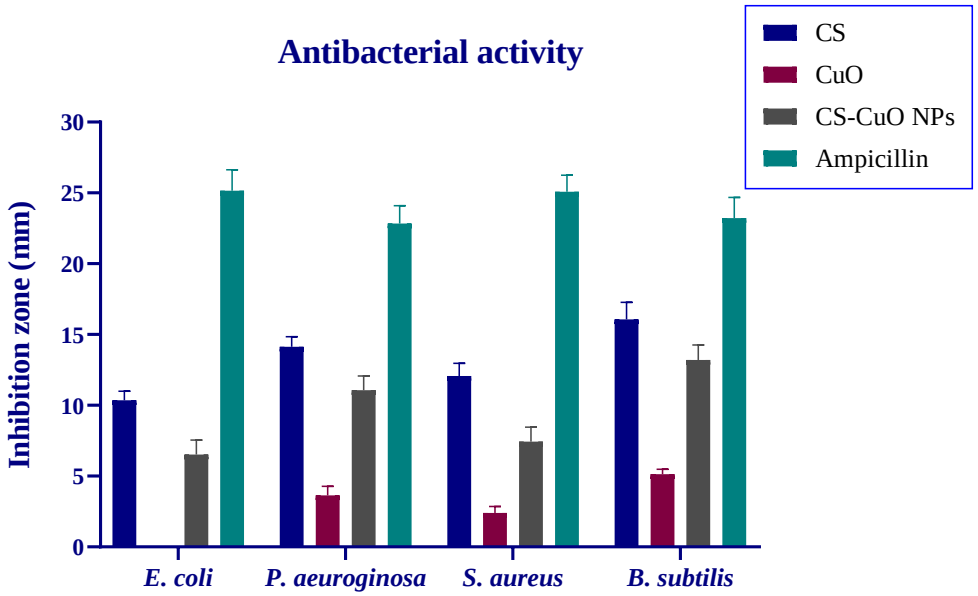

Fig. 5. Antibacterial activities of chitosan (CS), copper oxide (CuO) and chitosan-copper oxide nanoparticles (CS-CuO NPs) against 2 Gram-negative bacteria (*E. coli* and *P. aeuroginosa*) as well as 2 Gram-positive (*S. aureus* and *B. subtilis*). Ampicillin represents a positive control. Results are expressed as mean ± SD

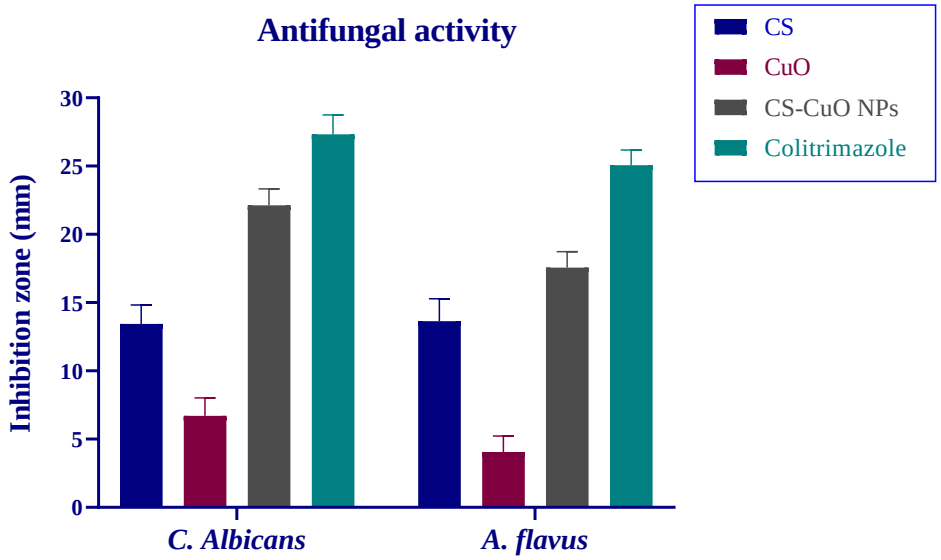

Fig. 6. Antifungal activities of chitosan (CS), copper oxide (CuO) and chitosan-copper oxide nanoparticles (CS-CuO NPs) against 2 fungal species (*C. Albicans* and *A. flavus*). Colitrimazole represents a positive control. Results are expressed as mean ± SD.

Antioxidant activities

1. DPPH radical scavenging assay

All tested compounds exhibited a potent antioxidant activity property in a dose dependent manner (Fig. 7). Overall, CS possessed the highest scavenging with a significant minimum IC_{50} value of 0.02± 0.001 mg/mL compared to that of CuO and CS-CuO NPs (0.09± 0.007 and 0.07± 0.004 mg/mL, respectively) (P< 0.001). Markedly, CS showed similar DPPH radical scavenging activity as vitamin C (standard antioxidant) with IC_{50} value = 0.023± 0.001 mg/mL, as compared to that of vitamin c (IC_{50} = 0.02± 0.001 mg/mL, P>0.05) (Table 4).

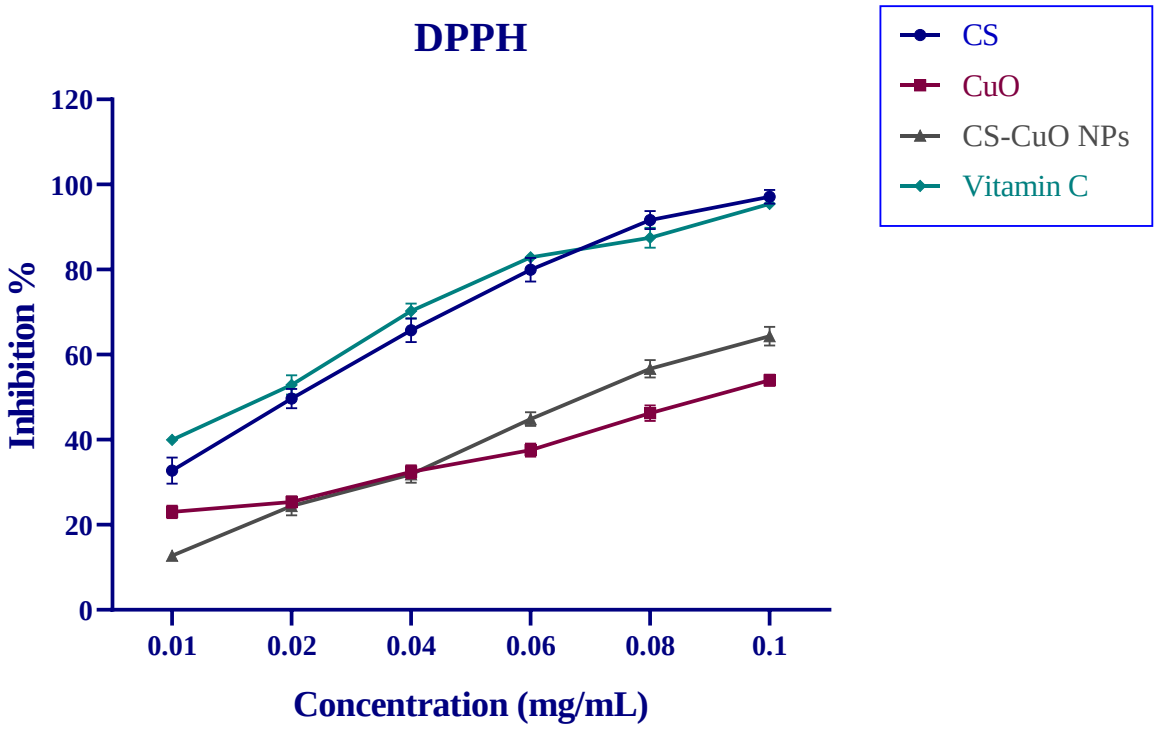

Fig. 7. Antioxidant activities of chitosan (CS), copper oxide (CuO) and chitosan-copper oxide nanoparticles (CS-CuO NPs) using DPPH radical scavenging assay. Vitamin C represents a positive control. Results are expressed as mean ± SD.

2. Ferric reducing antioxidant power (FRAP)

The reducing activity of the CS, CuO and CS-CuO NPs compounds for the ferric ion were assessed using FRAP assay. All tested compounds displayed concentration-dependent reducing power of ferric ions (Fig. 8). The assay revealed that the CS-CuO NPs displays the highest reducing capacity (82.94 % ± 1.42) at a concentration of 1 mg/mL compared with less reducing activity for CS (78.12% ±0.84) and CuO (70.46% ± 1.28) at the same concentration. The IC_{50} of the CS-CuO NPs in FRAP assays was

identified as = 0.17 ± 0.005 mg/mL, While, CuO and CS have higher IC_{50} values are 0.31± 0.01 and 0.2± 0.005 mg/mL, respectively (Table 4).

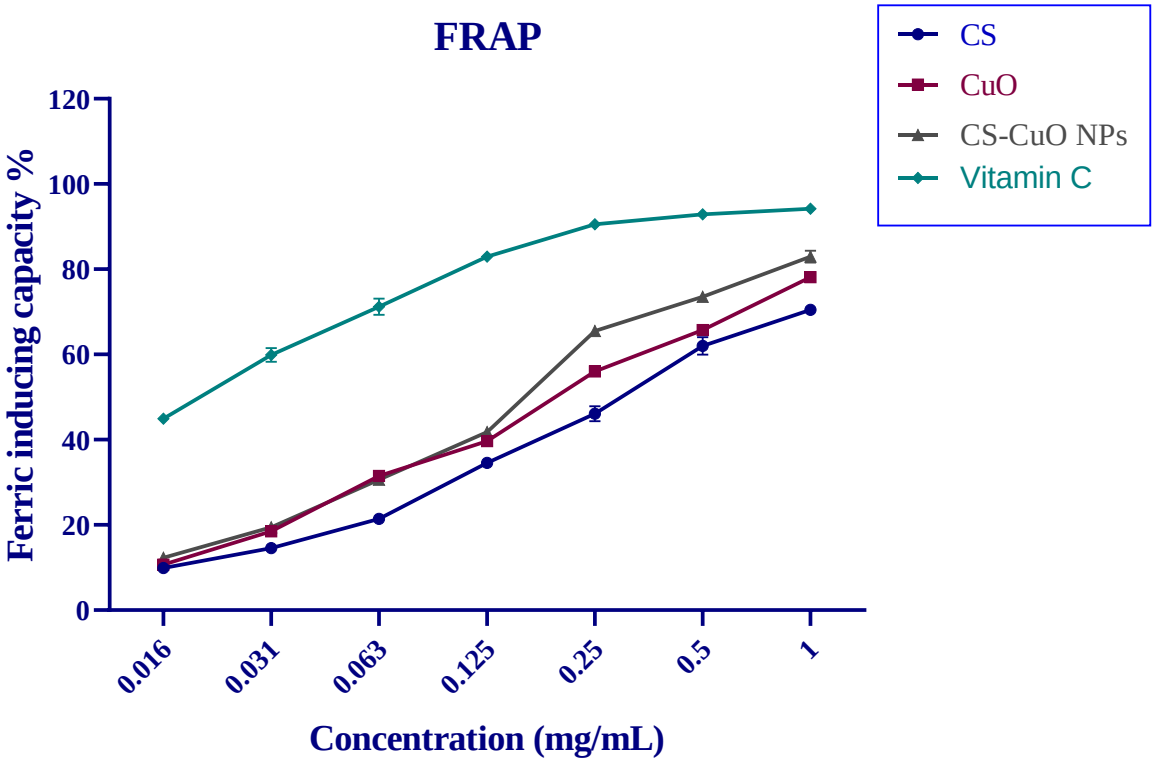

Fig. 8. Antioxidant activities of chitosan (CS), copper oxide (CuO) and chitosan-copper oxide nanoparticles (CS-CuO NPs) using FRAP assay. Vitamin C represents a positive control. Results are expressed as mean ± SD.

3. NO radical scavenging assay

The NO radical scavenging assay has been also employed to assess the antioxidant potency of CS, CuO and CS-CuO NPs compounds. As shown in Fig. (9), the scavenging activity for NO radicals all tested compounds were concentration dependent with highest scavenging activity of 76.81% ± 1.35 for at CS-CuO NPs a concentration of 1.0 mg/mL. Less scavenging effects were observed for CS and CuO at the same mentioned concentration with 70.36% ± 1.28 and 63.59 % ± 1.38, respectively. Further, the CS-CuO NPs displayed an IC_{50} of 0.21± 0.005 mg/mL, 50 and 100 % higher active than that of CuO and CS with IC_{50} 0.32± 0.001and 0.45± 0.011 mg/mL, respectively (Table 4).

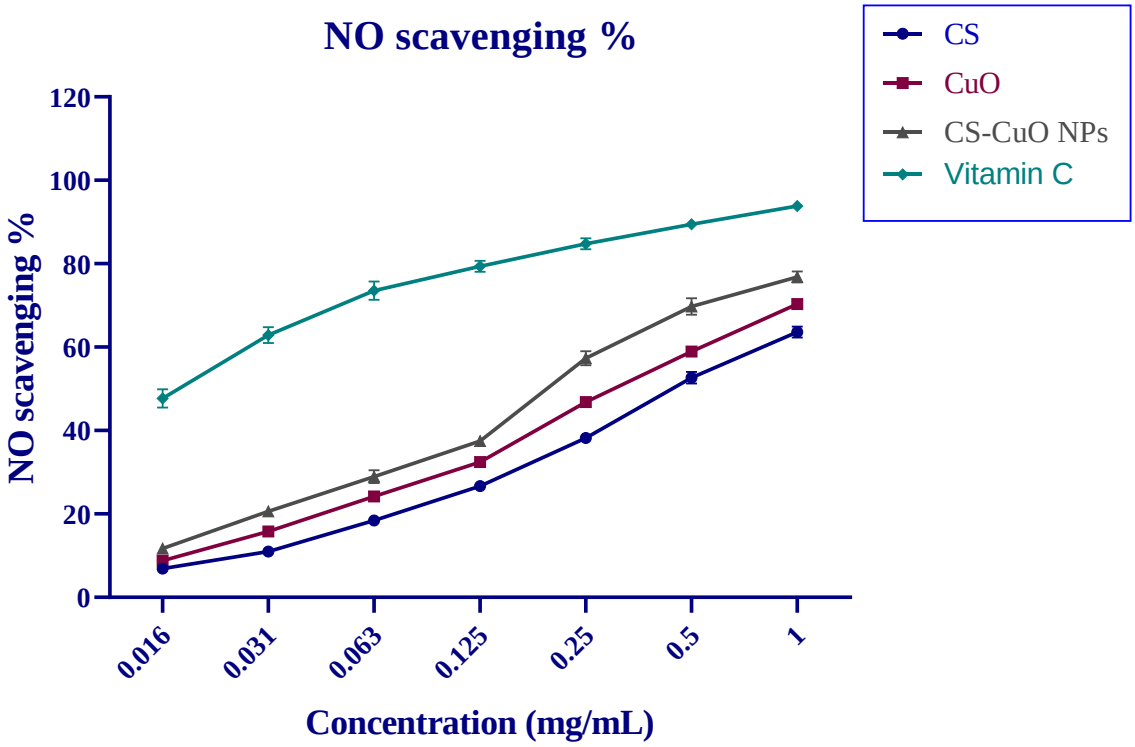

Fig. 9. Antioxidant activities of chitosan (CS), copper oxide (CuO) and chitosan-copper oxide nanoparticles (CS-CuO NPs) using NO scavenging assay. Vitamin C represents positive control. Results are represented as mean ± SD

Table 4. IC_{50} values of CS, CuO, CS-CuO NPs and vitamin C against DPPH, FRAP, and NO free radicals

	IC_{50} (mg/mL)		
	DPPH	**FRAP**	**NO**
CS	0.02±0.001	0.31±0.01	0.45±0.011
CuO	0.09±0.007	0.21±0.005	0.32±0.001
CS-CuO NPs	0.07±0.004	0.17±0.005	0.21±0.005
Vitamin C	0.02±0.001	0.02± 0.001	0.02±0.001

IC_{50} values are represented as means ± SD.

Anti-inflammatory activities (COX-2 inhibition assay)

To further evaluate the bioactivity of the most potent antioxidant compounds, CS and CS–CuO nanoparticles, their anti-inflammatory potential was assessed using a cyclooxygenase-2 (COX-2) enzyme inhibition assay. As shown in Fig. (10), both compounds demonstrated significant inhibitory effects on COX-2 activity in a dose-dependent manner. At a concentration of 1mg/ mL, CS and CS–CuO NPs achieved inhibition rates of 61.27% ± 1.91 and 52.31% ± 1.75, respectively.

Notably, CS–CuO NPs exhibited higher potency compared to CS, with an IC_{50} value of 0.57 ± 0.016 mg/mL, while CS displayed an IC_{50} of 0.91 ± 0.014 mg/mL. These results indicate that conjugation with CuO enhanced the inhibitory efficiency of CS against COX-2, highlighting the potential of CS–CuO nanocomposites as promising anti-inflammatory agents.

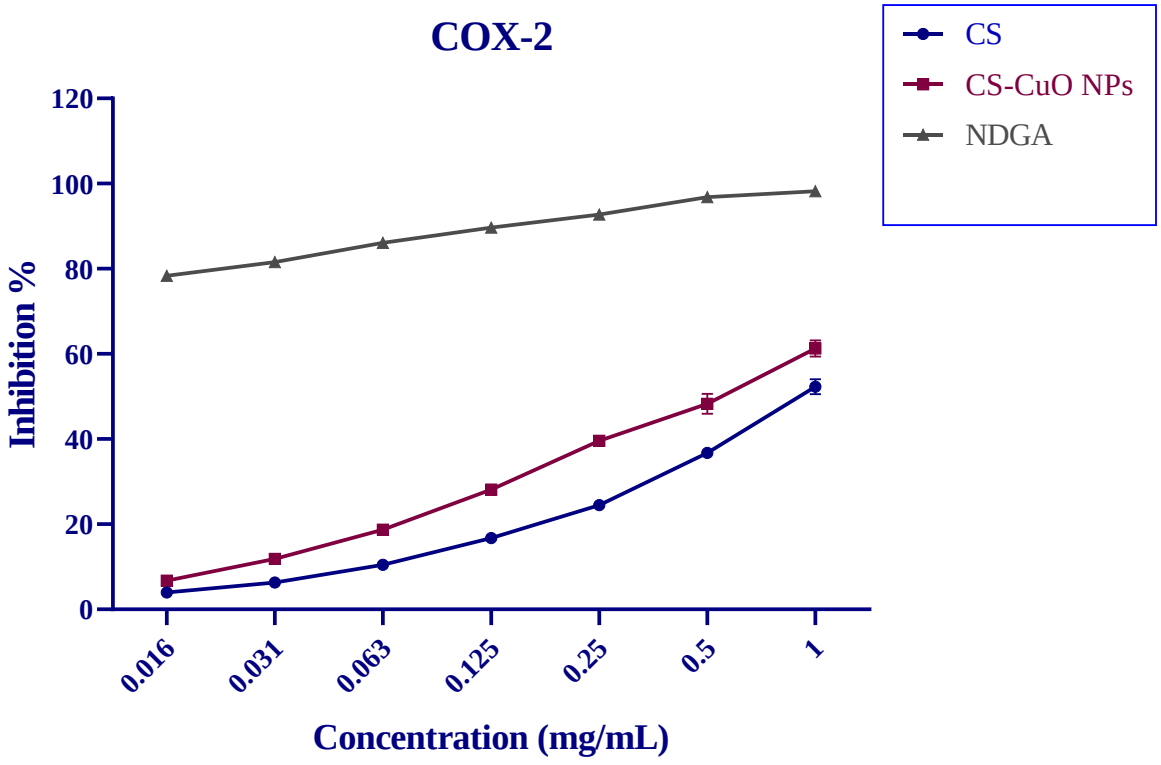

Fig. 10. Anti-inflammatory activities of chitosan (CS) and chitosan-copper oxide nanoparticles (CS-CuO NPs) using COX-2 inhibition assay. Nordihydroguairetic acid (NDGA) represents a standard. Results are represented as mean ± SD.

DISCUSSION

Marine bivalve molluscs are main functional groups in the marine ecosystems as they are water filters, consumers, biomarkers, food source rather their medical importance as rich source of bioactive agents **(Mesquita *et al*., 2023)**. *Mactra stultorum* is an edible marine bivalve molluscs used as a popular food supplement in the Mediterranean cities **(Derbali *et al*., 2021)**. As far as the authors' knowledge are aware, this study provides the first scientific evidence shedding light on the biometric relationships and biological activities of *Mactra stultorum* collected from Mediterranean Sea in Port Said, Egypt. According to **Lim *et al*. (2014)**, the allometric relationships are one of common tools used for the assessment of bivalve health condition that reflect their ability to adapt the environmental conditions. The obtained results from the relationships between SL-SH, SL-SWi and SL-SWt revealed that this bivalve species had a negative allometric growth ($b<1$) indicating that SH, SWi and SWt increase at a slower rate compared with the shell length. The relationship between SL and TWt in the current study displayed a positive allometric relationship ($b>3$). Similar results to the present study were revealed by **Gab-Alla *et al*. (2007)** where they showed the negative allometric relationships between SL-SH and SL-SWi and positive allometry between SL-TWt for *Mactera alarina* from two sites of Suez Bay, Egypt. In addition, **Farghaly *et al*. (2022)** showed that the shell length- total weight relationship of *Paphia textile*, collected from Suez Canal, Egypt, revealed a positive allometric growth pattern ($b > 3$). Other species of clams were also reported to have the same allometric relationship between shell length and total weight, and such reported data are consistent with the present findings **(Çolakoğlu & Palaz, 2014; Argente & Ilano, 2021)**. Along with the current findings , it has also been reported that SH, SWi and SWt increased in lower rate than SL (negative allomerty) in *Lithophaga lithophaga* **(Somaya *et al*., 2018)**. Such variations in the allometric growth of bivalves depend on local environmental factors, species and physiological traits **(Caill-Milly *et al*., 2012; Bensaâd-Bendjedid *et al*., 2017; Derbali *et al*., 2019, 2021, 2022)**. Interestingly, the obtained findings in the current study agree with the negative allometry obtained from SL-SH relationship for the same studied species in Tunis **(Derbali *et al*., 2021)**. However, this later study showed that the SL-SWi relationship was isometry and SL- TWt relationship was negative allometry; this outcome disagrees with our data. Environmental conditions like salinity, wave action, temperature and the availability of food resource can affect bivalve growth pattern **(O'connor & Lawler, 2004; Lodola *et al*., 2013; Zakzok *et al*., 2022)**.

The nanocomposite of chitosan-copper oxide nanoparticles in the current study was characterized by IR, X-ray powdered diffractions and TEM. IR indicated the loading of CS onto CuO, the spectrum of the free chitosan showed broad bands which are thought to arise from the symmetric and asymmetric stretching motions of amino groups ν (NH_2)

(**Queiroz *et al.*, 2015)**. The spectrum of CS-CuO showed stretching vibrations bands of the hydroxyl and amino groups in their positions as the free (CS) with slight shifts. The free CS showed a shoulder band at 1580cm^{-1}; these data may refereed to the in-plan-bending of the amino group δ(NH_2) **(Queiroz *et al.*, 2015)**. The broad band of free chitosan at 1263 and 1083 cm^{-1} due to the bond (C-O-C) and the in – plan-bending of the hydroxyl groups δ(OH), respectively **(Hosny *et al.*, 2016)**. The spectrum of (CS-CuO) showed two new bands at 523 and 609 cm^{-1} due to ν(Cu-N) and ν(CuO), respectively **(Hosny & El-Dossoki, 2008)**. It can be deduced that chitosan was loaded to CuO nanoparticles from the shifts of the bands which are among features of the free chitosan after loading onto CuO nanoparticles. XRD verified monoclinic CuO nanoparticles formation as the XRD pattern chitosan-copper oxide nanoparticles exhibited peaks between 20-30^{o}; these peaks have been reported earlier **(Kaur *et al.*, 2013)** for chitosan. This finding confirms the loading of chitosan onto CuO NPs. TEM images also showed the formation of CuO quantum dots with sizes around 5 nm.

The present study also evaluated the anti-tumor, ant-microbial and antioxidant activities of chitosan; a chitin derivative extracted from the shell of *M. stultorum.* Assessing the biological activities of CuO nanoparticles has been widely reported in a panel of scientific reports **(Rajamma *et al.*, 2020; Shwetha *et al.*, 2021)**. **Sarkar *et al.* (2012)** showed that a complex of metal oxide nanoparticle and organic or inorganic polymers can increase their biological effects. Contrarily, the present study showed that chitosan-copper oxide nanoparticles had higher cytotoxicity against HepG2 cell lines and fungal species than the other activities either of chitosan and CuO against the same cells. While chitosan was more cytotoxic and selective for MCF-7, HCT cell lines, Gram-positive and Gram-negative bacteria, as well considerable potent anti-oxidant activities. **Ke *et al.* (2021)** clarified that the biological effect of chitosan depends on the type of the treated cell and the physicochemical properties of functional groups of the chitosan such as C3-OH, C6-OH and C2-NH2. Hence, the physicochemical properties of some of chitosan functional groups may be affected or blocked when combined with CuO NPs leading to less anticancer (against breast and colon carcinoma cell lines), antibacterial and anti-oxidant (DPPH) activities of CS-CuO NPs than chitosan.

Similarly, chitosan anticancer activity has been commonly reported **(Almutairi *et al.*, 2020; Tuorkey *et al.*, 2022)**, coinciding with the current outputs, where all tested compounds showed prominent anticancer effects against studied cell lines. The highest cytotoxic effect against HepG2 cell lines was obtained following the treatment by CS-CuO NPs which is consistent with the finding of **Sarfraz *et al.* (2023)** who compared the inhibitory effect of CS, CuO and CS-CuO NPs against HepG2 cell lines. In the present study, chitosan had the lowest IC_{50} value on breast and colon carcinoma cell lines; moreover, **Abdelwahab *et al.* (2020)** synthesized composites of chitosan that had a potential cytotoxicity against MCF-7 and HCT-116 cell lines. According to **Ding and**

Guo (2022), chitosan and its derivatives can induce apoptosis of different cancer cells by increasing the mitochondrial membrane potential, ROS levels and calcium ions concentration. Various signaling pathways related to progression of cancer can also be modulated by chitosan, including PI3K/Akt/mTOR pathway **(Amirani *et al*., 2020)**, MAPK/ERK pathway **(Chen *et al*., 2022)** and the NF-κB pathway **(Herdiana *et al*., 2023)**.

The present study pointed to the prominent antimicrobial, antioxidant, and anticancer activities of copper oxide which is consistent with several reports **(Gawande *et al*., 2016; Makvandi *et al*., 2020; Priya *et al*., 2020; Rafieyan *et al*., 2022)**. These activities of copper oxide (CuO) may be attributed to the presence of a hydroxyl radical on its surface which may damage cell membranes and biological processes by producing reactive species **(Prabhu & Poulose, 2012; Dizaj *et al*., 2014; Meghana *et al*., 2015, Bhadra, 2019)**. However, in the current study, CuO had the lowest effects compared with the biological effects chitosan and chitosan-copper oxide nanoparticles.

The negative charge of the microbial membrane and the positive charge of CS, CuO and CS-CuO NPs interact electrostatically causing blockage of nutrient intake by the microbial cells leading to their growth inhibition **(Haldorai & Shim, 2013)**. In addition, the electrostatic interaction can enhance intracellular oxidative stress in the microbial cells **(Applerot *et al*., 2012)**. In the present study, the potential of the anti-bacterial activity against studied bacteria was in the order of CS> CS-CuO NPs>Cuo. In this respect, **Andres *et al*. (2007)** reported the potential inhibitory effect of chitosan on *P. aeruginosa, E. coli, S. saprophyticus* and *E. faecalis;* they proposed that the free amino groups of chitosan could cause bacterial cell wall disruption. The permeability of the microbial cell membrane increases depend on the electrostatic interaction between the positive charge of chitosan and the negative charge of the microbial cell membrane interact electrostatically and this disrupt the balance of the internal osmotic causing inhibition of microorganisms' growth **(Nagy *et al*., 2011)**. **Sudarshan *et al*. (1992)** revealed the potential antibacterial properties of chitosan as only low concentrations of chitosan lead to permeabilization of bacterial cell. In contrast with our results, **Javed *et al*. (2021)** reported that CS-CuO NPs had the highest antibacterial activity followed by CuO and chitosan had the lowest activity. **Umoren *et al*. (2022)** showed that olive leaf extract- mediated CH-CuO nanoparticles had a potential antibacterial effect against *P. aeruginosa, E. coli*, *S. haemolytica* and *B. cereus*. **Paul *et al*. (2023)** also reported that CS-CuO NPs had a significant antibacterial activity against gram-positive as well as gram-negative bacteria. Different studies have reported that CuO nanoparticles exert antibacterial effect, especially against drug-resistant bacteria **(Azam *et al*., 2012a, b; Dadi *et al*., 2019)**.

The anti-fungal activity against *Candida albicans* and *Aspergillus flavus* was evaluated in the current study and the potential activity was in the order of CS-CuO NPs>CS>CuO. **Sondi and Salopek-Sondi (2004)** illustrated that the antifungal activity of nanoparticle is usually associated with their small size facilitating their penetration through the membrane of microbial cells. A ddditionally, **Ahmed *et al*. (2021)** reported the antifungal activity of CS-CuO NPs against fungus *C. albican* and *C. neoformans*. **Lo *et al*. (2020)** studied the antifungal activity of different types of chitosan against *C. tropicalis* and *C. albicans*; they also reported the potential synergism between chitosan and fluconazole. Furthermore, the antifungal activity of chitosan has been widely recorded in prior studies **(Balicka-Ramisz *et al*., 2005; Tipparat & Oraphan, 2008)**. CuO nanoparticles were reported to inhibit the growth of *A. Niger, C. albican* and *C. clavus* **(Bhadra, 2019)**.

Oxidative damage to vital cellular components can be triggered by the imbalance between the antioxidant enzymes and molecules in the body and the free radicals. Oxidative damage has adverse consequences on the body where it can induce many of critical diseases **(Jakubczyk *et al*., 2020; Yan & Allen, 2021; Murphy *et al*., 2022; Di Bona *et al*., 2024)**. Antioxidants include molecules that suppress the toxic effects of free radicals **(Cerdá *et al*., 2014; Nwachukwu *et al*., 2021; Zakzok *et al*., 2022)**. Antioxidant capacity can be measured by NO assay through which free radicals can be inactivated through a hydrogen atom release by the possible antioxidant agents; DPPH and FRAP assays measure the transfer or the release of an electron to a free radical which converts it into an anion **(Shahidi & Zhong, 2015; Platzer *et al*., 2021; Zakzok *et al*., 2021)**. In the present study, CS exhibited the highest antioxidant capacity through DPPH assay while CS-CuO-NPs had the highest antioxidant capacity through FRAP and NO assays, this may be related to the difference in the reaction conditions of different assays **(Oyaizu, 1986; Marcocci *et al*., 1994; Brand-Williams *et al*., 1995)**. Previous studies indicated the anti-oxidant activity of chitosan **(Yen *et al*., 2008; Cerdá *et al*., 2014; Wölfle *et al*., 2014)**. Amino and hydroxyl groups of chitosan can donate hydrogen ions that lead to scavenge free radicals **(Castro Marín *et al*., 2019; Ivanova & Yaneva, 2020; Muthu *et al*., 2021)**. Moreover, the random distribution of amino groups enables them to generate inter- and intra-molecular hydrogen bonds **(Ngo & Kim, 2014)**. The activity of a nano material as an anti-oxidant is one of the most important targets in the nano science. It is well reported that CuO nanoparticles had an anti-oxidant activity **(Dobrucka, 2018)**. The electron density of CuO nanoparticles can be transferred to the free radicals **(Das *et al*., 2013)**. In comparison with CS and CuO, previous studies showed that CS-CuO-NPs biocomposites had the highest ability to scavenge radicals; Synergistic effect of CS-CuO-NPs biocomposite may be the reason why the antioxidant activity increased **(Revathi & Thambidurai, 2019; Sarfraz *et al*., 2023)**.

The activated COX-2 enzyme enhances the generation of the inflammatory prostaglandins that can trigger chronic inflammation **(Kaur & Singh, 2022)**. Therefore, the inhibition of such enzyme reduces the inflammation and indicates an anti-inflammatory activity of the inhibitory agents **(Bertolini *et al*., 2002; Ahmadi *et al*., 2022; Ju *et al*., 2022)**. The present study revealed that CS-CuO NPs inhibit COX-2 enzyme. Consistently, several reports indicated the anti-inflammatory activity of chitosan **(Lee *et al*., 2006; Friedman *et al*., 2013; Pandiyan *et al*., 2022)**. Chitosan can inhibit NF-κB pathway and can abolish the synthesis of TNF-α which promotes the COX-2 expression **(Ma *et al*., 2016; Chang *et al*., 2019)**. Metal oxides such as CuO, when combined with chitosan in the form of nanoparticles, most of biological activities are enhanced **(Adhikari & Yadav, 2018; Sarfraz *et al*., 2023)**. Previous studies have illustrated the anti-inflammatory activity of chitosan- metal oxide NPs **(Tian *et al*., 2021; Elmehbad *et al*., 2023; Elhabal *et al*., 2024)**.

CONCLUSION

The present work investigated the biometric relationships of *Mactra stultorum*; the results displayed both negative and positive allometric growth, which reflects that the bivalve grows in non-ideal environmental conditions. In addition, The present study evaluated the anticancer, antimicrobial, antioxidant, and anti-inflammatory activities of CS, CuO and CS-CuO NPs. In the term of comparison, CS and CS-CuO NPs displayed the most potent activities compared to CuO. Additionally, the potency of either CS or CS-CuO NPs exhibited a variation in different experiments. Furthermore, this study suggested that the difference in the potential effects between CS and CS-CuO NPs was related to the type of the treated cells, availability and physiochemical properties of chitosan functional groups.

REFERENCES

AbdElhady, M.M. (2012). Preparation and Characterization of Chitosan/Zinc Oxide Nanoparticles for Imparting Antimicrobial and UV Protection to Cotton Fabric. International Journal of Carbohydrate Chemistry, 2012: 1–6. https://doi.org/10.1155/2012/840591

Abdelwahab, H.E.; Yacout, G.A. and El Sadek, M.M. (2020). Cytotoxicity influence of new chitosan composite on HEPG-2, HCT-116 and MCF-7 carcinoma cells. International Journal of Biological Macromolecules, 158: 1102–1109. https://doi.org/10.1016/j.ijbiomac.2020.04.253

Adhikari, H.S. and Yadav, P.N. (2018). Anticancer Activity of Chitosan, Chitosan Derivatives, and Their Mechanism of Action. International Journal of Biomaterials, 2018: 1–29. https://doi.org/10.1155/2018/2952085

Agarwal, M.; Agarwal, M.K.; Shrivastav, N.; Pandey, S.; Das, R. and Gaur, P. (2018). Preparation of Chitosan Nanoparticles and their *In-vitro* Characterization. IJLSSR., 4: 1713–1720. https://doi.org/10.21276/ijlssr.2018.4.2.17

Ahmadi, M.; Bekeschus, S.; Weltmann, K.; Woedtke, T. and Wende, K. (2022). Non-steroidal anti-inflammatory drugs: recent advances in the use of synthetic COX-2 inhibitors. RSC Medicinal Chemistry, 13: 471. https://doi.org/10.1039/d1md00280e

Ahmed, S.B.; Mohamed, H.I.; Al-Subaie, A.M.; Al-Ohali, A.I. and Mahmoud, N.M. (2021). Investigation of the antimicrobial activity and hematological pattern of nano-chitosan and its nano-copper composite. Sci Rep., 11: 9540. https://doi.org/10.1038/s41598-021-88907-z

Almutairi, F.M.; El Rabey, H.A.; Tayel, A.A.; Alalawy, A.I.; Al-Duais, M.A.; Sakran, M.I. and Zidan, N.S. (2020). Augmented anticancer activity of curcumin loaded fungal chitosan nanoparticles. Int J Biol Macromol., 155: 861–867. https://doi.org/10.1016/j.ijbiomac.2019.11.207

Amirani, E.; Hallajzadeh, J.; Asemi, Z.; Mansournia, M.A. and Yousefi, B. (2020). Effects of chitosan and oligochitosans on the phosphatidylinositol 3-kinase-AKT pathway in cancer therapy. International Journal of Biological Macromolecules, 164: 456–467. https://doi.org/10.1016/j.ijbiomac.2020.07.137

Andres, Y.; Giraud, L.; Gerente, C. and Le Cloirec, P. (2007). Antibacterial effects of chitosan powder: mechanisms of action. Environ Technol., 28: 1357–1363. https://doi.org/10.1080/09593332808618893

Applerot, G.; Lellouche, J.; Lipovsky, A.; Nitzan, Y.; Lubart, R.; Gedanken, A. and Banin, E. (2012). Understanding the Antibacterial Mechanism of CuO Nanoparticles: Revealing the Route of Induced Oxidative Stress. Small, 8: 3326–3337. https://doi.org/10.1002/smll.201200772

Argente, F.A. and Ilano, A. (2021). Population dynamics and aquaculture potential of the mud clam, *Geloina expansa* (Mousson, 1849) (Bivalvia: Cyrenidae) in loay-loboc river, Bohol, Central Philippines. Journal of Sustainability Science and Management, 16: 43–55. https://doi.org/10.46754/jssm.2021.04.004

Azam, A.; Ahmed, A.S.; Oves, M.; Khan, M.S.; Habib, S.S. and Memic, A. (2012a). Antimicrobial activity of metal oxide nanoparticles against Gram-positive and Gram-negative bacteria: a comparative study. International Journal of Nanomedicine, 7: 6003. https://doi.org/10.2147/IJN.S35347

Azam, A.; Ahmed, A.S.; Oves, S.; Khan, M.S. and Memic, A. (2012b). Size-dependent antimicrobial properties of CuO nanoparticles against Gram-positive and -negative bacterial strains. IJN., 7: 3527–3535. https://doi.org/10.2147/IJN.S29020

Azuma, K.; Ifuku, S.; Osaki, T.; Okamoto, Y. and Minami, S. (2014). Preparation and Biomedical Applications of Chitin and Chitosan Nanofibers. j biomed nanotechnol., 10: 2891–2920. https://doi.org/10.1166/jbn.2014.1882

Balicka-Ramisz, A.; Wojtasz-Pajak, A.; Pilarczyk, B.; Ramisz, A. and Laurans, L. (2005). Antibacterial and antifungal activity of chitosan. Proceedings of 12th International Congress on Animal Hygene, 2.

Barreto, M.S.; Andrade, C.T.; Azero, E.G.; Paschoalin, V.M. and Del Aguila, E.M. (2017). Production of Chitosan/Zinc Oxide Complex by Ultrasonic Treatment with Antibacterial Activity. J Bacteriol Parasitol., 8. https://doi.org/10.4172/2155-9597.1000330

Bauer, A.W.; Kirby, W.M.; Sherris, J.C. and Turck, M. (1966). Antibiotic susceptibility testing by a standardized single disk method. Am J Clin Pathol., 45: 493–496.

Bensaâd-Bendjedid, L.; Belhaouas, S.; Kerdoussi, A.; Djebbari, N.; Tahri, M. and Bensouilah, M. (2017). Age, growth, mortality and condition index of an unexploited Ruditapes decussatus population from El Mellah lagoon Algeria. Int. J. Biosci., 11: 436–442. https://doi.org/10.12692/ijb/11.1.436-442

Bertolini, A.; Ottani, A. and Sandrini, M. (2002). Selective COX-2 inhibitors and dual acting anti-inflammatory drugs: critical remarks. Curr Med Chem., 9: 1033–1043. https://doi.org/10.2174/0929867024606650

Bhadra, P. (2019). CuO and CuO@SiO_2 as a potential antimicrobial and anticancer drug. Journal of Microbiology, Biotechnology and Food Sciences, 9: 63–69. https://doi.org/10.15414/jmbfs.2019.9.1.63-69

Brand-Williams, W.; Cuvelier, M. E. and Berset, C. (1995). Use of a free radical method to evaluate antioxidant activity. LWT - Food Science and Technology., 28: 25–30. https://doi.org/10.1016/S0023-6438(95)80008-5

Caill-Milly, N.; Bru, N.; Mahé, K.; Borie, C. and D′Amico, F. (2012). Shell Shape Analysis and Spatial Allometry Patterns of Manila Clam (*Ruditapes philippinarum*) in a Mesotidal Coastal Lagoon. Journal of Marine Sciences, 2012: 281206. https://doi.org/10.1155/2012/281206

Castro Marín, A.; Culcasi, M.; Cassien, M.; Stocker, P.; Thétiot-Laurent, S.; Robillard, B.; Chinnici, F. and Pietri, S. (2019). Chitosan as an antioxidant alternative to sulphites in oenology: EPR investigation of inhibitory mechanisms. Food Chem., 285: 67–76. https://doi.org/10.1016/j.foodchem.2019.01.155

Cerdá, C.; Sánchez, C.; Climent, B.; Vázquez, A.; Iradi, A.; El Amrani, F.; Bediaga, A. and Sáez, G.T. (2014). Oxidative stress and DNA damage in obesity-related tumorigenesis. Adv Exp Med Biol., 824: 5–17. https://doi.org/10.1007/978-3-319-07320-0_2

Chai, T.T.; Law, Y.C.; Wong, F.C. and Kim, S.K. (2017). Enzyme-Assisted Discovery of Antioxidant Peptides from Edible Marine Invertebrates: A Review. Mar Drugs., 15: 42. https://doi.org/10.3390/md15020042

Chang, S.H.; Lin, Y.Y.; Wu, G.J.; Huang, C.H. and Tsai, G.J. (2019). Effect of chitosan molecular weight on anti-inflammatory activity in the RAW 264.7

macrophage model. Int J Biol Macromol., 131: 167–175. https://doi.org/10.1016/j.ijbiomac.2019.02.066

Chen, J.; Zhou, Z.; Zheng, C.; Liu, Y.; Hao, R.; Ji, X.; Xi, Q.; Shen, J. and Li, Z. (2022). Chitosan oligosaccharide regulates AMPK and STAT1 pathways synergistically to mediate PD-L1 expression for cancer chemoimmunotherapy. Carbohydr Polym., 277: 118869. https://doi.org/10.1016/j.carbpol.2021.118869

Chernikov, O.; Kuzmich, A.; Chikalovets, I.; Molchanova, V. and Hua, K.F. (2017). Lectin CGL from the sea mussel *Crenomytilus grayanus* induces Burkitt's lymphoma cells death via interaction with surface glycan. Int J Biol Macromol., 104: 508–514. https://doi.org/10.1016/j.ijbiomac.2017.06.074

Çolakoğlu, S. and Palaz, M. (2014). Some population parameters of *Ruditapes philippinarum* (Bivalvia, Veneridae) on the southern coast of the Marmara Sea, Turkey. Helgol Mar Res., 68: 539–548. https://doi.org/10.1007/s10152-014-0410-7

Covarrubias, C.; Trepiana, D. and Corral, C. (2018). Synthesis of hybrid copper-chitosan nanoparticles with antibacterial activity against cariogenic *Streptococcus mutans* . Dental Materials Journal, 37: 379–384. https://doi.org/10.4012/dmj.2017-195

Dadi, R.; Azouani, R.; Traore, M.; Mielcarek, C. and Kanaev, A. (2019). Antibacterial activity of ZnO and CuO nanoparticles against gram positive and gram negative strains. Materials Science and Engineering, 104: 109968. https://doi.org/10.1016/j.msec.2019.109968

Das, D.; Nath, B.C.; Phukon, P. and Dolui, S.K. (2013). Synthesis and evaluation of antioxidant and antibacterial behavior of CuO nanoparticles. Colloids and Surfaces B: Biointerfaces, 101: 430–433. https://doi.org/10.1016/j.colsurfb.2012.07.002

Derbali, A.; Hadj Taieb, A. and Jarboui, O. (2021). Stock Size Assessment, Distribution and Biology of the Surf Clam *Mactra stultorum* (Mollusca: Bivalvia) Along the Sfax Coasts (Tunisia, Mediterranean Sea). Thalassas, 37: 781–789. https://doi.org/10.1007/s41208-021-00352-x

Derbali, A.; Hashem, K.; Taieb, A. and Jarboui, O. (2022). Population dynamics of the cockle *Cerastoderma glaucum* (Mollusca: Bivalvia) in the Gulf of Gabes (Tunisia). ANNALES. Ser. hist. nat., 32: 431–442. https://doi.org/10.19233/ASHN.2022.ŠT

Derbali, A.; Kandeel, K.E. and Jarboui, O. (2019). Comparison of the Dynamics between Coastal and Midshore Populations of *Pinctada radiata* (Leach, 1814) (Mollusca: Bivalvia) in the Gulf of Gabes, Tunisia. TrJFAS., 20: 301–310.

Di Bona, M.; Chen, Y.; Agustinus, A.S.; Mazzagatti, A.; Duran, M.A.; Deyell, M.; Bronder, D.; Hickling, J.; Hong, C.; Scipioni, L.; Tedeschi, G.; Martin, S.; Li, J.; Ruzgaitė, A.;, Riaz, N.; Shah, P.; D'Souza, E.K.; Brodtman, D.Z.; Sidoli, S.; Diplas, B.; Jalan, M.; Lee, N.Y.; Ordureau, A.; Izar, B.; Laughney, A.M.; Powell, S.; Gratton, E.; Santaguida, S.; Maciejowski, J.; Ly, P.;

Jeitner, T.M. and Bakhoum, S.F. (2024). Micronuclear collapse from oxidative damage. Science., 385: eadj8691. https://doi.org/10.1126/science.adj8691

Ding, J. and Guo, Y. (2022). Recent Advances in Chitosan and its Derivatives in Cancer Treatment. Frontiers in Pharmacology, 13: 888740. https://doi.org/10.3389/fphar.2022.888740

Dizaj, S.M.; Lotfipour, F.; Barzegar-Jalali, M.; Zarrintan, M.H. and Adibkia, K. (2014). Antimicrobial activity of the metals and metal oxide nanoparticles. Materials Science and Engineering: C., 44: 278–284. https://doi.org/10.1016/j.msec.2014.08.031

Dobrucka, R. (2018). Antioxidant and Catalytic Activity of Biosynthesized CuO Nanoparticles Using Extract of Galeopsidis herba. J Inorg Organomet Polym., 28: 812–819. https://doi.org/10.1007/s10904-017-0750-2

Elhabal, S.F.; Abdelaal, N.; Al-Zuhairy, S.A.K.; Elrefai, M.F.M.; Hamdan, A.M.; Khalifa, M.M.; Hababeh, S.; Khasawneh, M.A.; Khamis, G.M.; Nelson, J.; Mohie, P.M.; Gad, R.A.; Rizk, A.; Kabil, S.L.; El-Ashery, M.K.; Jasti, B.R.; Elzohairy, N.A.; Elnawawy, T.; Hassan, F.E. and El-Nabarawi, M.A. (2024). Green Synthesis of Zinc Oxide Nanoparticles from *Althaea officinalis* Flower Extract Coated with Chitosan for Potential Healing Effects on Diabetic Wounds by Inhibiting TNF-α and IL-6/IL-1β Signaling Pathways. Int J Nanomedicine., 19: 3045–3070. https://doi.org/10.2147/IJN.S455270

Elieh-Ali-Komi, D. and Hamblin, M.R. (2016). Chitin and Chitosan: Production and Application of Versatile Biomedical Nanomaterials. Int J Adv Res (Indore)., 4: 411–427.

Elmehbad, N.Y.; Mohamed, N.A.; Abd El-Ghany, N.A. and Abdel-Aziz, M.M. (2023). Evaluation of the *in vitro* anti-inflammatory and anti-*Helicobacter pylori* activities of chitosan-based biomaterials modified with copper oxide nanoparticles. International Journal of Biological Macromolecules, 253: 127277. https://doi.org/10.1016/j.ijbiomac.2023.127277

Farghaly, M.I.; El-Sayed Ali, T.; Mitwally, H.M. and Abdel Razek, F.A. (2022). First insight into the growth and population aspects of the carpet clam *Paphia textile* (Gmelin, 1791), the main bivalve species along the Suez Canal, Egypt. Egyptian Journal of Aquatic Research, 48: 265–272. https://doi.org/10.1016/j.ejar.2022.06.003

Ferreira, M.; Lago, J.; Vieites, J.M. and Cabado, A.G. (2014). World Production of Bivalve Mollusks and Socioeconomic Facts Related to the Impact of Marine Biotoxins, in: Seafood and Freshwater Toxins. CRC Press.

Friedman, A.J.; Phan, J.; Schairer, D.O.; Champer, J.; Qin, M.; Pirouz, A.; Blecher-Paz, K.; Oren, A.; Liu, P.T.; Modlin, R.L. and Kim, J. (2013). Antimicrobial and Anti-Inflammatory Activity of Chitosan–Alginate

Nanoparticles: A Targeted Therapy for Cutaneous Pathogens. Journal of Investigative Dermatology, 133: 1231–1239. https://doi.org/10.1038/jid.2012.399

Gab-Alla, A.A.F.; Mohamed, S.Z.; Mahmoud, M.A.M. and Soliman, B.A. (2007). Ecological and Biological Studies on Some Economic Bivalves in Suez Bay, Gulf of Suez, Red Sea, Egypt. Journal of Fisheries and Aquatic Science, 2: 178–194. https://doi.org/10.3923/jfas.2007.178.194

Gawande, M.B.; Goswami, A.; Felpin, F.X.; Asefa, T.; Huang, X.; Silva, R.; Zou, X.; Zboril, R. and Varma, R.S. (2016). Cu and Cu-Based Nanoparticles: Synthesis and Applications in Catalysis. Chem Rev., 116: 3722–3811. https://doi.org/10.1021/acs.chemrev.5b00482

Gouda, M. and Hebeish, A. (2010). Preparation and Evaluation of CuO/Chitosan Nanocomposite for Antibacterial Finishing Cotton Fabric. Journal of Industrial Textiles, 39: 203–214. https://doi.org/10.1177/1528083709103142

Hahn, T.; Tafi, E.; Paul, A.; Salvia, R.; Falabella, P. and Zibek, S. (2020). Current state of chitin purification and chitosan production from insects. Journal of Chemical Technology & Biotechnology, 95: 2775–2795. https://doi.org/10.1002/jctb.6533

Haldorai, Y. and Shim, J.J. (2013). Multifunctional Chitosan-Copper Oxide Hybrid Material: Photocatalytic and Antibacterial Activities. International Journal of Photoenergy, 2013: 245646. https://doi.org/10.1155/2013/245646

Hasan, I.; Gerdol, M.; Fujii, Y.; Rajia, S.; Koide, Y.; Yamamoto, D.; Kawsar, S. and Ozeki, Y. (2016). cDNA and Gene Structure of MytiLec-1, A Bacteriostatic R-Type Lectin from the Mediterranean Mussel (*Mytilus galloprovincialis*). Mar Drugs., 14: 92. https://doi.org/10.3390/md14050092

Herdiana, Y.; Wathoni, N.; Gozali, D.; Shamsuddin, S. and Muchtaridi, M. (2023). Chitosan-Based Nano-Smart Drug Delivery System in Breast Cancer Therapy. Pharmaceutics, 15: 879. https://doi.org/10.3390/pharmaceutics15030879

Hosny, N.M. and El-Dossoki, F.I. (2008). Schiff Base Complexes Derived from 2-Acetylpyridine, Leucine, and Some Metal Chlorides: Their Preparation, Characterization, and Physical Properties. J. Chem. Eng. Data., 53: 2567–2572. https://doi.org/10.1021/je800415n

Hosny, N.M.; Zoromba, M.S.; Samir, G. and Alghool, S. (2016). Synthesis, structural and optical properties of Eskolaite nanoparticles derived from Cr doped polyanthranilic acid (CrPANA). Journal of Molecular Structure, 1122: 117–122. https://doi.org/10.1016/j.molstruc.2016.05.071

Ivanova, D.G. and Yaneva, Z.L. (2020). Antioxidant Properties and Redox-Modulating Activity of Chitosan and Its Derivatives: Biomaterials with Application in Cancer Therapy. BioResearch Open Access, 9: 64. https://doi.org/10.1089/biores.2019.0028

Jakubczyk, K.; Dec, K.; Kałduńska, J.; Kawczuga, D.; Kochman, J. and Janda, K. (2020). Reactive oxygen species - sources, functions, oxidative damage. Pol Merkur Lekarski., 48: 124–127.

Javed, R.; Rais, F.; Kaleem, M.; Jamil, B.; Ahmad, M.A.; Yu, T.; Qureshi, S.W. and Ao, Q. (2021). Chitosan capping of CuO nanoparticles: Facile chemical preparation, biological analysis, and applications in dentistry. International Journal of Biological Macromolecules, 167: 1452–1467. https://doi.org/10.1016/j.ijbiomac.2020.11.099

Ju, Z.; Li, M.; Xu, J.; Howell, D.C.; Li, Z. and Chen, F.E. (2022). Recent development on COX-2 inhibitors as promising anti-inflammatory agents: The past 10 years. Acta Pharmaceutica Sinica., 12: 2790. https://doi.org/10.1016/j.apsb.2022.01.002

Kaur, B. and Singh, P. (2022). Inflammation: Biochemistry, cellular targets, anti-inflammatory agents and challenges with special emphasis on cyclooxygenase-2. Bioorg Chem., 121: 105663. https://doi.org/10.1016/j.bioorg.2022.105663

Kaur, P.; Choudhary, A. and Thakur, R. (2013). Synthesis of Chitosan-Silver Nanocomposites and their Antibacterial Activity, 4.

Ke, C.L.; Deng, F.S.; Chuang, C.Y. and Lin, C.H. (2021). Antimicrobial Actions and Applications of Chitosan. Polymers, 13: 904. https://doi.org/10.3390/polym13060904

Klug, H.P. and Alexander, L.E. (1974). X-Ray Diffraction Procedures: For Polycrystalline and Amorphous Materials, 2nd Edition. Wiley (accessed 11.1.24).

Larsen, L.N.; Dahl, E. and Bremer, J. (1996). Peroxidative oxidation of leuco-dichlorofluorescein by prostaglandin H synthase in prostaglandin biosynthesis from polyunsaturated fatty acids. Biochim Biophys Acta., 1299: 47–53. https://doi.org/10.1016/0005-2760(95)00188-3

Lastovina, T.; Budnyk, A.; Khaishbashev, G.; Kudryavtsev, E. and Soldatov, A. (2016). Copper-based nanoparticles prepared from copper (II) acetate bipyridine complex. J Serb Chem Soc., 81: 751–762. https://doi.org/10.2298/JSC151211036L

Lee, C.G.; Da Silva, C.A.; Dela Cruz, C.S.; Ahangari, F.; Ma, B.; Kang, M.J.; He, C.H.; Takyar, S. and Elias, J.A. (2011). Role of Chitin and Chitinase/Chitinase-Like Proteins in Inflammation, Tissue Remodeling, and Injury. Annu Rev Physiol., 73: 10.1146/annurev-physiol-012110–142250. https://doi.org/10.1146/annurev-physiol-012110-142250

Lee, D.W.; Shirley, S.A.; Lockey, R.F. and Mohapatra, S.S. (2006). Thiolated chitosan nanoparticles enhance anti-inflammatory effects of intranasally delivered theophylline. Respiratory Research, 7: 112. https://doi.org/10.1186/1465-9921-7-112

Lim, H.J.; Lim, M.S.; Lee, W.Y.; Choi, E.H.; Yoon, J.H.; Park, S.Y.; Lee, S.M. and Kim, S.K. (2014). Condition index and hemocyte apoptosis as a health indicator for the Pacific oysters, *Crassostrea gigas* cultured in the western coastal waters of

Korea. The Korean Journal of Malacology, 30: 189–196. https://doi.org/10.9710/kjm.2014.30.3.189

Lingaraju, K.; Naika, H.R.; Nagabhushana, H.; Jayanna, K.; Devaraja, S. and Nagaraju, G. (2019). Biosynthesis of nickel oxide nanoparticles from Euphorbia heterophylla (L.) and their biological application. Arabian Journal of Chemistry, 13(3): 4712–4719. https://doi.org/10.1016/j.arabjc.2019.11.003

Lo, W.H.; Deng, F.S.; Chang, C.J. and Lin, C.H. (2020). Synergistic Antifungal Activity of Chitosan with Fluconazole against Candida albicans, Candida tropicalis, and Fluconazole-Resistant Strains. Molecules, 25: 5114. https://doi.org/10.3390/molecules25215114

Lodola, A.; Nicolini, L.; Savini, D.; Deidun, A. and Occhipinti-Ambrogi, A. (2013). Range expansion and biometric features of *Pinctada imbricata radiata* (Bivalvia: Pteriidae) around Linosa Island, Central Mediterranean Sea (Italy). Italian Journal of Zoology, 80: 303–312. https://doi.org/10.1080/11250003.2013.775363

Ma, L.; Shen, C.A.; Gao, L.; Li, D.W.; Shang, Y.R.; Yin, K.; Zhao, D.X.; Cheng, W.F. and Quan, D.Q. (2016). Anti-inflammatory activity of chitosan nanoparticles carrying NF-κB/p65 antisense oligonucleotide in RAW264.7 macropghage stimulated by lipopolysaccharide. Colloids Surf B Biointerfaces., 142: 297–306. https://doi.org/10.1016/j.colsurfb.2016.02.031

Makvandi, P.; Wang, C.; Zare, E.N.; Borzacchiello, A.; Niu, L. and Tay, F.R. (2020). Metal-Based Nanomaterials in Biomedical Applications: Antimicrobial Activity and Cytotoxicity Aspects. Advanced Functional Materials, 30: 1910021. https://doi.org/10.1002/adfm.201910021

Marcocci, L.; Maguire, J.J.; Droylefaix, M.T. and Packer, L. (1994). The Nitric Oxide-Scavenging Properties of Ginkgo Biloba Extract EGb 761. Biochemical and Biophysical Research Communications, 201: 748–755. https://doi.org/10.1006/bbrc.1994.1764

Meghana, S.; Kabra, P.; Chakraborty, S. and Padmavathy, N. (2015). Understanding the pathway of antibacterial activity of copper oxide nanoparticles. RSC Adv., 5: 12293–12299. https://doi.org/10.1039/C4RA12163E

Mercan, N.; Kivrak, I.; Duru, M.E.; Katircioglu, H.; Gulcan, S.; Malci, S.; Acar, G. and Salih, B. (2006). Chemical composition effects onto antimicrobial and antioxidant activities of propolis collected from different regions of Turkey. Ann. Microbiol., 56: 373–378. https://doi.org/10.1007/BF03175035

Mesquita, F.; Gonçalves, F. and Gonçalves, A. (2023). Marine Bivalves' Ecological Roles and Humans-Environmental Interactions to Achieve Sustainable Aquatic Ecosystems. https://doi.org/10.5772/intechopen.111386

Mosmann, T. (1983). Rapid colorimetric assay for cellular growth and survival: application to proliferation and cytotoxicity assays. J. Immunol. Methods., 65: 55–63. https://doi.org/10.1016/0022-1759(83)90303-4

Murphy, M.P.; Bayir, H.; Belousov, V.; Chang, C.J.; Davies, K.J.A.; Davies, M.J.; Dick, T.P.; Finkel, T.; Forman, H.J.; Janssen-Heininger, Y.; Gems, D.; Kagan, V.E.; Kalyanaraman, B.; Larsson, N.G.; Milne, G.L.; Nyström, T.; Poulsen, H.E.; Radi, R.; Van Remmen, H.; Schumacker, P.T.; Thornalley, P.J.; Toyokuni, S.; Winterbourn, C.C.; Yin, H. and Halliwell, B. (2022). Guidelines for measuring reactive oxygen species and oxidative damage in cells and *in vivo*. Nat Metab., 4: 651–662. https://doi.org/10.1038/s42255-022-00591-z

Muthu, M.; Gopal, J.; Chun, S.; Devadoss, A.J.P.; Hasan, N. and Sivanesan, I. (2021). Crustacean Waste-Derived Chitosan: Antioxidant Properties and Future Perspective. Antioxidants, 10: 228. https://doi.org/10.3390/antiox10020228

Nagy, A.; Harrison, A.; Sabbani, S.; Munson, R.S.; Dutta, P.K. and Waldman, W.J. (2011). Silver nanoparticles embedded in zeolite membranes: release of silver ions and mechanism of antibacterial action. Int J Nanomedicine., 6: 1833–1852. https://doi.org/10.2147/IJN.S24019

Ngo, D.H. and Kim, S.K. (2014). Antioxidant Effects of Chitin, Chitosan, and Their Derivatives, in: Advances in Food and Nutrition Research. Elsevier, pp. 15–31. https://doi.org/10.1016/B978-0-12-800268-1.00002-0

Nwachukwu, I.D.; Sarteshnizi, R.A.; Udenigwe, C.C. and Aluko, R.E. (2021). A Concise Review of Current *In Vitro* Chemical and Cell-Based Antioxidant Assay Methods. Molecules, 26: 4865. https://doi.org/10.3390/molecules26164865

O'connor, W.A. and Lawler, N.F. (2004). Reproductive condition of the pearl oyster, *Pinctada imbricata*, Röding, in Port Stephens, New South Wales, Australia. Aquaculture Research, 35: 385–396. https://doi.org/10.1111/j.1365-2109.2004.01027.x

Odeleye, T.; Li, Y.; White, W.L.; Nie, S.; Chen, S.; Wang, J. and Lu, J. (2016). The antioxidant potential of the New Zealand surf clams. Food Chem., 204: 141–149. https://doi.org/10.1016/j.foodchem.2016.02.120

Oyaizu, M. (1986). Studies on Products of Browning Reaction: Antioxidative Activities of Products of Browning Reaction Prepared from Glucosamine. The Japanese Journal of Nutrition and Dietetics, 44: 307–315. https://doi.org/10.5264/eiyogakuzashi.44.307

Pandiyan, I.; Rathinavelu, P.K.; Arumugham, M.I. and Balasubramaniam, A. (2022). Efficacy of Chitosan and Chlorhexidine Mouthwash on Dental Plaque and Gingival Inflammation: A Systematic Review. Cureus., 14: e23318. https://doi.org/10.7759/cureus.23318

Paul, S.; M.K., D. and Peter, S. (2023). Development of Green Synthesized Chitosan-coated Copper Oxide Nanocomposite Gel for Topical Delivery. J Pharm Innov., 18: 1010–1019. https://doi.org/10.1007/s12247-022-09701-6

Perelshtein, I.; Ruderman, E.; Perkas, N.; Tzanov, T.; Beddow, J.; Joyce, E.; Mason, T.J.; Blanes, M.; Mollá, K.; Patlolla, A.; Frenkel, A.I. and Gedanken,

A. (2013). Chitosan and chitosan–ZnO-based complex nanoparticles: formation, characterization, and antibacterial activity. J. Mater. Chem. B 1., 1968. https://doi.org/10.1039/c3tb00555k

Platzer, M.; Kiese, S.; Herfellner, T.; Schweiggert-Weisz, U.; Miesbauer, O. and Eisner, P. (2021). Common Trends and Differences in Antioxidant Activity Analysis of Phenolic Substances Using Single Electron Transfer Based Assays. Molecules, 26: 1244. https://doi.org/10.3390/molecules26051244

Prabhu, S. and Poulose, E.K. (2012). Silver nanoparticles: mechanism of antimicrobial action, synthesis, medical applications, and toxicity effects. Int Nano Lett., 2: 32. https://doi.org/10.1186/2228-5326-2-32

Priya, D.D.; Khan, M.R. and Roopan, S.M. (2020). Fabricating a g-C3N4/CuO heterostructure with improved catalytic activity on the multicomponent synthesis of pyrimidoindazoles. J Nanostruct Chem., 10: 289–308. https://doi.org/10.1007/s40097-020-00350-0

Queiroz, M.F.; Melo, K.R.; Sabry, D.A.; Sassaki, G.L. and Rocha, H.A. (2015). Does the Use of Chitosan Contribute to Oxalate Kidney Stone Formation? Marine Drugs, 13: 141–158. https://doi.org/10.3390/md13010141

Rafieyan, S.G.; Marahel, F.; Ghaedi, M. and Maleki, A. (2022). Application of Terminalia catappa wood-based activated carbon modified with CuO nanostructures coupled with H_2O_2 for the elimination of chemical oxygen demand in the gas refinery. J Nanostruct Chem., 12: 159–177. https://doi.org/10.1007/s40097-021-00409-6

Rajamma, R.; Gopalakrishnan, S.; Abdul Khadar, F. and Baskaran, B. (2020). Antibacterial and anticancer activity of biosynthesised CuO nanoparticles. IET Nanobiotechnol., 14: 833–838. https://doi.org/10.1049/iet-nbt.2020.0088

Revathi, T. and Thambidurai, S. (2019). Cytotoxic, antioxidant and antibacterial activities of copper oxide incorporated chitosan-neem seed biocomposites. International Journal of Biological Macromolecules, 139: 867–878. https://doi.org/10.1016/j.ijbiomac.2019.07.214

Sarfraz, M.H.; Zubair, M.; Aslam, B.; Ashraf, A.; Siddique, M.H.; Hayat, S.; Cruz, J.N.; Muzammil, S.; Khurshid, M.; Sarfraz, M.F.; Hashem, A.; Dawoud, T.M.; Avila-Quezada, G.D. and Abd-Allah, E.F. (2023). Comparative analysis of phyto-fabricated chitosan, copper oxide, and chitosan-based CuO nanoparticles: antibacterial potential against *Acinetobacter baumannii* isolates and anticancer activity against HepG2 cell lines. Front. Microbiol., 14. https://doi.org/10.3389/fmicb.2023.1188743

Sarkar, S.; Guibal, E.; Quignard, F. and SenGupta, A.K. (2012). Polymer-supported metals and metal oxide nanoparticles: synthesis, characterization, and applications. J Nanopart Res., 14: 715. https://doi.org/10.1007/s11051-011-0715-2

Shahidi, F. and Zhong, Y. (2015). Measurement of antioxidant activity. Journal of Functional Foods, Natural Antioxidants, 18: 757–781. https://doi.org/10.1016/j.jff.2015.01.047

Shwetha, U.R.; Latha, M.S.; Kumar, C.R.; Kiran, M.S.; Onkarappa, H.S. and Betageri, V.S. (2021). Potential antidiabetic and anticancer activity of copper oxide nanoparticles synthesised using Areca catechu leaf extract. Adv. Nat. Sci: Nanosci. Nanotechnol., 12: 025008. https://doi.org/10.1088/2043-6262/ac0448

Somaya, M.T.; Abdel Razek, F.A.; Khafage, A.R.; Omar, H.A. and El-Deeb, R.S. (2018). Biometric variables and relative growth of the date mussel Lithophaga lithophaga (L., 1758) (Bivalvia: Mytilidae) from the Eastern Mediterranean Sea, Egypt. Egyptian Journal of Aquatic Biology & Fisheries, 22: 241–248. https://doi.org/10.21608/ejabf.2018.22062

Sondi, I. and Salopek-Sondi, B. (2004). Silver nanoparticles as antimicrobial agent: a case study on E. coli as a model for Gram-negative bacteria. J Colloid Interface Sci., 275: 177–182. https://doi.org/10.1016/j.jcis.2004.02.012

Souza, V.G.; Rodrigues, C.; Valente, S.; Pimenta, C.; Pires, J.R.; Alves, M.M.; Santos, C.F.; Coelhoso, I.M. and Fernando, A.L. (2020). Eco-Friendly ZnO/Chitosan Bionanocomposites Films for Packaging of Fresh Poultry Meat. Coatings, 10: 110. https://doi.org/10.3390/coatings10020110

Sudarshan, N.R.; Hoover, D.G. and Knorr, D. (1992). Antibacterial action of chitosan. Food Biotechnology, 6(3): 257–272. https://doi.org/10.1080/08905439209549838

Syame, S.M.; Mohamed, W.S.; Mahmoud, R.K. and Omara, S.T. (2017). Synthesis of Copper-Chitosan Nanocomposites and their Applications in Treatment of Local Pathogenic Isolates Bacteria. Orient. J. Chem., 33: 2959–2969. https://doi.org/10.13005/ojc/330632

Teissier, G. (1948). The allometric relationship; its statistical and biological significance. Biometrics, 4.

Thomas, N.V.; Venkatesan, J.; Manivasagan, P. and Kim, S.K. (2015). Production and Biological Activities of Chitooligosaccharides (COS)-An Overview. Journal of Chitin and Chitosan Science, 3: 1–10. https://doi.org/10.1166/jcc.2015.1084

Tian, Z.; Chinnathambi, A.; Awad, T.; Krishna, S.; Priya, V. and Kumar, S. (2021). Anti-arthritic activity of Tin oxide-Chitosan-Polyethylene glycol carvacrol nanoparticles against Freund's adjuvant induced arthritic rat model via the inhibition of cyclooxygenase-2 and prostaglandin E2. Arabian Journal of Chemistry, 14: 103293. https://doi.org/10.1016/j.arabjc.2021.103293

Tipparat, H. and Oraphan, R. (2008). Effect of deacetylation conditions on antimicrobial activity of chitosans prepared from carapace of black tiger shrimp (*Penaeus monodon*). Songklanakarin Journal of Science and Technology, 30.

Tuorkey, M.; Khedr, Y.; Aborhyem, S. and Xue, X. (2022). Green synthesis of chicory (*Cichorium intybus* L.) Chitosan nanoparticles and evaluation of their

anti-fungal, anti-hemolytic, and anti-cancer activities. Journal of Bioactive and Compatible Polymers, 37: 421–436. https://doi.org/10.1177/08839115221126737

Umoren, P.S.; Kavaz, D.; Nzila, A.; Sankaran, S.S. and Umoren, S.A. (2022). Biogenic Synthesis and Characterization of Chitosan-CuO Nanocomposite and Evaluation of Antibacterial Activity against Gram-Positive and -Negative Bacteria. Polymers, 14: 1832. https://doi.org/10.3390/polym14091832

Wijsman, J.; Troost, K.; Fang, J. and Roncarati, A. (2019). Global Production of Marine Bivalves. Trends and Challenges, in: Smaal, A.C., Ferreira, J.G., Grant, J., Petersen, J.K., Strand. (Eds.), Goods and Services of Marine Bivalves. Springer International Publishing, Cham., 7–26. https://doi.org/10.1007/978-3-319-96776-9_2

Wölfle, U.; Seelinger, G.; Bauer, G.; Meinke, M.C.; Lademann, J. and Schempp, C.M. (2014). Reactive molecule species and antioxidative mechanisms in normal skin and skin aging. Skin Pharmacol Physiol., 27: 316–332. https://doi.org/10.1159/000360092

Yan, L.J. and Allen, D.C. (2021). Cadmium-Induced Kidney Injury: Oxidative Damage as a Unifying Mechanism. Biomolecules, 11: 1575. https://doi.org/10.3390/biom11111575

Yen, M.T.; Yang, J.H. and Mau, J.L. (2008). Antioxidant properties of chitosan from crab shells. Carbohydrate Polymers, 74: 840–844. https://doi.org/10.1016/j.carbpol.2008.05.003

Zakzok, S.M.; Abd El-ghany, A.G.; Anas, A.Y.; Dahshan, S.K.; Rashad, M.E.; Yasser, M. and Tawfik, M.M. (2022). Biometric study, sex ratio and potential biological activities of the edible mantis shrimp *Erugosquilla massavensis*. Egyptian Journal of Aquatic Biology and Fisheries, 26: 229–253. https://doi.org/10.21608/ejabf.2022.249663

Zakzok, S.M.; Alkaradawe, R.M.; Mohammad, S.H. and Tawfik, M.M. (2021). Antiproliferative and antioxidant activities of the edible crab *Callinectes sapidus* hepatopancreas and hemolymph extracts. Egyptian Journal of Aquatic Biology and Fisheries, 25: 531–550. https://doi.org/10.21608/ejabf.2021.179659

Zakzok, S.M.; Tawfik, M.M.; Mohammad, S.H. and Alkaradawe, R.M. (2022). Biometric Study, Condition Factor and Biochemical Composition of the Blue Crab *Callinectes sapidus* Rathbun, 1896. Journal of Fisheries and Environment, 46: 100–115.